

REMOVAL OF PERFLUOROOCCTANOIC ACID USING ZEROVALENT
IRON BASED MATERIALS

By

WASIU ADEDAPO LAWAL

DISSERTATION

Submitted in partial fulfillment of the requirements
for the degree of Doctor of Philosophy at
The University of Texas at Arlington
Department of Earth and Environmental Sciences
May 2018

Arlington, Texas

Supervising Committee:

Hyeok Choi, Supervising Professor
Max Hu
Andrew Hunt
Junha Jeon
Melanie Sattler

ABSTRACT

Removal of Perfluorooctanoic Acid Using Zerovalent Iron Based Materials

Wasiu Adedapo Lawal, Ph.D

University of Texas at Arlington, 2018

Supervising Professor: Hyeok Choi

Perfluorinated alkyl substances (PFASs) are highly persistent organic contaminants that have become a global health concern. Few studies so far have demonstrated successful decomposition of PFASs under ambient condition. As a result, this feasibility study aimed to quickly examine whether or not zerovalent iron (ZVI)-based materials, in particular palladium-doped nanoscale ZVI (so-called nZVI/Pd) known to dehalogenate many halogenated chemicals, can remove perfluorooctanoic acid (PFOA) in water, one of the most widely used PFASs. Batch experiments were performed to evaluate the effects of various operating parameters including reaction pH, nZVI/Pd dose, and PFOA concentration, and thus to find best treatment options for PFOA. Significant removal of PFOA was observed at low pH and high nZVI/Pd dosage while nZVI/Pd was superior to micron-size ZVI and nZVI without Pd. However, decrease in total organic carbon was very similar to PFOA removal, negligible amounts of fluoride ions were detected in water, and mass spectrometry analysis indicated no significant formation of reaction intermediates. The results implied that the observed PFOA removal was more closely associated with adsorption than reaction (i.e., defluorination). Kinetic models and adsorption isotherm models were employed to explain the PFOA removal and obtain insights on the physicochemical processes around nZVI/Pd interacting with PFOA.

ACKNOWLEDGMENTS

Many thanks go to Allah for giving me the strength and intellect to do something like this and also for surrounding me with a support system that has helped keep me together all these years.

Next, I would like to thank Dr. Hyeok Choi for accepting me as his student and for guiding me through my research. The other members of my Ph.D. committee also deserve many thanks: Dr. Andrew Hunt, Dr. Melanie Sattler, Dr. Max Hu and Dr. Junha Jeon.

I would like to express my gratitude to all the colleagues I have had during this journey, most especially Akshay Parenky and Naomi Gevaerd de Souza, as well as Prince Nfodzo, Abolfazl Zakersalehi, Hesam Zamankhan and Celyna Karitas Olivera da Silva Rackov. Thank you all for your help and comradeship in the lab. This also includes all Environmental Engineering graduate students. I also want to thank my friend Eugenia Narh for being a co-conspirator on many of my extracurricular activities at UTA and also for being a friend outside the walls of campus as well.

I want to express my deep appreciation to Dr. Marietta Richard for all her advice that helped me stay motivated during these tough times. Special thanks also go to various members of staff who have helped in various ways, Larisa Koumanitskaya, Sara Ridnour, Tracy Pior, Paul Shover, Kierra David Godfrey, Lisa Berry, Brenda Davis, Dr. Raymond Jackson, Dr. Jim Grover. UT Arlington President Dr. Vistasp Karbhari also deserves special thanks for his wise leadership and encouragement.

Special thanks go to my parents, not just for the gift of genetics and intellect but also for nurturing and guiding me and leading me to become the person that I am at this moment.

Lastly and most importantly, I want to thank my wife and children for making the biggest sacrifice that has allowed me to take the time off other duties to work on my Ph.D. I appreciate your sacrifices and promise to make up for it in no time.

DEDICATION

To Taibat, Nadiyyah and Aaliyyah for being my inspiration.

To the poor people across the globe who don't have access to clean water.

TABLE OF CONTENTS

ABSTRACT	ii
ACKNOWLEDGMENTS	iii
DEDICATION	v
LIST OF TABLES	ix
LIST OF FIGURES	x
CHAPTER 1	1
Introduction and Literature Review	1
1.1 Chemistry	1
1.2 Synthesis.....	3
1.3 Usage.....	4
1.4 Occurrence	5
1.5 Health Concerns/Toxicity	6
1.6 Environmental Regulations	7
1.7 Analytical Techniques.....	9
1.8 Current Treatment Methods	12
1.9 Nanomaterials and water treatment.....	22
1.10 Nanoscale zerovalent Iron (nZVI).....	23
1.11 Objectives of this study	29
CHAPTER 2	30

Methodology	30
2.1 Chemicals and reagents	30
2.2 Preparation of nanoscale ZVI/Pd particles	30
2.3 Batch reaction procedures	31
2.4 Sample cleanup (solid phase extraction)	32
2.5 HPLC Analyses	34
2.6 Ion chromatography analysis	38
2.7 Total organic carbon measurements	40
2.8 LC-MS/MS measurements	42
2.9 Zeta potential analysis	43
2.10 Physical characterization of iron particles	45
2.11 Calculations	45
CHAPTER 3	46
Results	46
3.1 Physical properties of nZVI particles	46
3.2 Comparison of ZVI Materials	48
3.2 Effects of Reaction pH, nZVI/Pd Dose, and PFOA Concentration	50
3.3 Results on TOC, MS/MS, and Fluoride	53
3.4 PFOA Removal Kinetics and Mechanisms	56
CHAPTER 5	65

Conclusion and future work.....	65
References.....	67

LIST OF TABLES

Table 1.1. Physico-chemical properties of PFOA	2
Table 1.2 Physico-chemical properties of PFOS	2
Table 1.3. Analytical methods for the determination of PFASs in aqueous matrices	11
Table 1.4. Physical sorption of PFOA and PFOS from selected literature	14
Table 1.5. Reductive degradation of PFASs in selected literature	17
Table 1.6. Oxidative decomposition of PFASs from selected literature	21
Table 1.7. Properties of various nZVI particles synthesized by different methods	25
Table 2.1 Gradient program for PFOA identification by HPLC with suppressed conductivity detection	25
Table 3.1 Comparison of Rate Constants and Calculated q_e Values of the Kinetic Models at Various Initial Concentrations of PFOA (5 g/L nZVI/Pd and pH 5).....	51
Table 3.2 Calculated isotherm constants for the Freundlich, Langmuir and Chapman isotherms	53

LIST OF FIGURES

Figure 1.1 Molecular structures of (a) PFOS and (b) PFOA	1
Figure 1.2 Schematic representation of fluorinated surfactants.....	2
Figure 1.3 Timeline of PFASs in the United States (Morrison 2016a)	8
Figure 1.4 Schematic representation of palladium doped nanoscale iron	27
Figure 2.1 HPLC Chromatogram of PFOA, (a.) without SPE, (b.) with SPE.....	33
Figure 2.2 SPE Apparatus.....	34
Figure 2.3 Flow diagram of the HPLC process from the Chemstation software.....	35
Figure 2.4 Flow diagram of the HPLC process from the Chemstation software.....	37
Figure 2.5 HPLC- Conductivity Detection Setup	38
Figure 2.6 Ion chromatography setup	39
Figure 2.7 Ion Chromatogram of 7 common anion standards	40
Figure 2.8 Total organic carbon instrument.....	41
Figure 2.9 LC-MS/MS instrumentation.....	42
Figure 2.10 Zeta potential/particle size analyzer	43
Figure 2.11 High power sonicator	44
Figure 3.1 X-ray diffraction patterns of (a) microscale ZVI (b) nanoscale ZVI.	46
Figure 3.2 High resolution transmission electron microscopic images of (a) microscale ZVI. (b) nanoscale ZVI.....	47
Figure 3.3 Fast Fourier Transform (FFT) diffraction pattern for a. microscale ZVI and b. nanoscale ZVI.....	47
Figure 3.4 Effect of various ZVI particles on PFOA removal (20 mg/L PFOA, 5 g/L ZVI materials, and pH 5).....	49

Figure 3.5. 0-minute (control) sample (a.) and 3-hour sample (b.) of 5 g/L nZVI/Pd. 20 mg/L PFOA	50
Figure 3.6 PFOA removal at various initial pHs (20 mg/L PFOA and 5 g/L nZVI/Pd).	51
Figure 3.7 PFOA removal at various nZVI/Pd concentrations (20 mg/L PFOA and pH 5).....	52
Figure 3.8 PFOA removal at various PFOA concentrations (5 g/L nZVI/Pd and pH 5).....	53
Figure 3.9. Effect of various ZVI particles on TOC removal (20 mg/L PFOA, 5 g/L ZVI materials, and pH 5	54
Figure 3.10. LC-MS/MS of PFOA reactor sample	55
Figure 3.11 Adsorption of PFOA onto nZVI/Pd at various PFOA concentrations (5 g/L nZVI/Pd and pH 5).....	57
Figure 3.12 Isotherm of PFOA adsorption onto nZVI/Pd	59
Figure 3.13 Zeta potential graphs of (a) nZVI and (b) nZVI/Pd	61
Figure 3.14 Zeta potential of nZVI and nZVI/Pd over pH	62
Figure 3.15 Schematic diagram of a surfactant bilayer on a positively charged surface.....	63

CHAPTER 1

Introduction and Literature Review

1.1 Chemistry

Perfluoroalkyl compounds (PFASs) are compounds that have alkyl chains but with all the hydrogen atoms replaced by fluorine atoms (Rayne and Forest 2009). They are part of the larger group of fluorinated alkyl compounds where at least one hydrogen has been substituted by a fluorine atom (Knepper and Lange 2011; Lange, Schmidt, and Brauch 2006). Typically, PFASs have the molecular formula $CF_3(CF_2)_nR$, where R could be any functional group such as hydroxyl, carboxylic acid or sulfonic acid among a few other possibilities (Knepper and Lange 2011; Rayne and Forest 2009). Among the most widely known PFASs are two compounds that each contain eight carbon atoms- perfluorooctanoic acid (PFOA, $C_7F_{15}COOH$) and Perfluorooctanesulfonic acid (PFOS, $C_8F_{17}SO_2OH$) which as would be discussed later, have found usage in quite a few applications (Benford et al. 2008; Renner 2001; Kissa 1994; Moody and Field 2000; Knepper and Lange 2011).

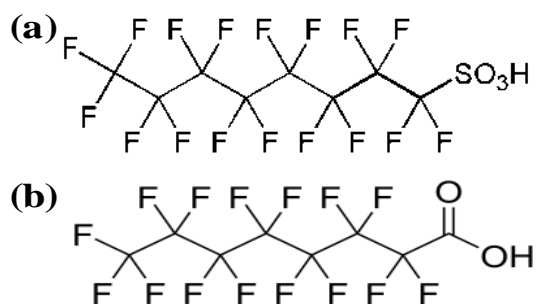


Figure 1.1 Molecular structures of (a) PFOS and (b) PFOA

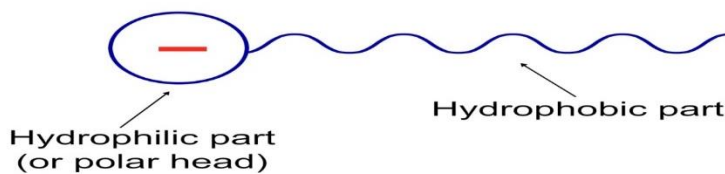


Figure 1.2 Schematic representation of fluorinated surfactants

Table 1.1 Physico-chemical properties of PFOA (H. Park et al. 2011, 1945-1953)

CAS Number	335-67-1
Molecular Weight	414 g/mol
Solubility	3.7 g/L
pK_a	<0.5
Critical Micellar Concentration	~30 mM
K_{aw}	1.02*10 ⁻³
Vapor Pressure (at 25 °C)	1.33 ×10 ³ Pa

Table 1.2 Physico-chemical properties of PFOS (H. Park et al. 2011)

CAS Number	1763-23-1
Molecular Weight	500
Solubility	0.519 g/L
pK_a	-3.27
Critical Micellar Concentration	~2 mM
K_{aw}	2*10 ⁻⁶
Vapor Pressure (at 25 °C)	3.31 × 10 ⁴ Pa

PFOA and PFOS are basically fluorinated surfactants and from their respective structures shown in Figure 1.1, they have a hydrophobic tail (fluorinated chain) and a hydrophilic head (the acidic functional groups) as represented in Figure 1.2. They are both also oleophobic. In fact, like other fluorinated surfactants, PFOA and PFOS have a much greater surface activity than their corresponding alkyl surfactants (Rayne and Forest 2009; Knepper and Lange 2011). Up to 100 times better in some cases.

Another significant property of PFASs is that they are, for the most part, chemically and thermally stable and for this reason, they are commonly referred to as persistent organic pollutants (POPs) (Z. Zhang et al. 2014; Bao et al. 2014; Teng, Tang, and Ou 2009; Arvaniti et al. 2015). This is obviously because of the abundance of fluorine atoms, given that with bond strength of 485 kJ/mol, the C-F bond is the strongest bond known in organic chemistry (O'Hagan 2008). One particular test showed that they remained stable in harsh environments such as hot, concentrated sulfuric acid, hydrofluoric acid and hot concentrated alkaline solutions whereas other kinds of surfactant would have been destroyed (Knepper and Lange 2011).

1.2 Synthesis

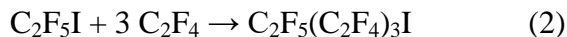
PFASs are generally anthropogenic, which means that their existence in the environment is mostly man-made. PFOA and PFOS are often synthesized via two main routes. Electrochemical fluorination (ECF) and telomerization (Kissa 1994; Knepper and Lange 2011). In electrochemical fluorination, an octanoyl chloride is dispersed in anhydrous hydrofluoric acid and exposed to electric current (5-7 volts) (Pabon and Corpart 2002, 149-156). This results in hydrogen being

evolved and being replaced by fluorine atoms to produce a perfluorinated acid chloride (as one of many products) which is then hydrolyzed to yield PFOA (Pabon and Corpart 2002). This is represented in equation 1 below.



For PFOS, an alkyl sulfonyl fluoride is the starting material instead, along with anhydrous hydrofluoric acid and the resulting perfluoroalkyl sulfonyl fluoride then undergoes hydrolysis to yield the final product. This method is widely used on a large scale and for industrial purposes.

With telomerization, PFASs can be “constructed” by using 2-carbon moieties and adding an acid or sulfonate group (for PFOA or PFOS respectively) at the end. Although telomerization yields fewer side products (and more of the targeted product), it is not widely used except for the production of PFOA and PFOS analytical standards.



1.3 Usage

Historically, chemical giants 3M and Dupont have been the major producers of PFOA and PFOS in the United States. 3M started producing PFOA in 1947 at its plant in Cottage Grove Minnesota while DuPont started using it in 1951 to produce Teflon. As of the year 2000, the production of these chemicals in the United States alone reached about 6.5 million pounds. One of the earliest reported uses of PFOA was in fabrics and leather products as a water and oil repellent although it is believed to no longer be the used for this purpose. It is also used for the production of fluoroacrylic esters which are commonly used in optical fibers, coatings and

membranes (Kudo et al. 2006; Kudo and Kawashima 2003). The sodium or potassium salt form of PFOA is used to produce useful fluoropolymers such as polytetrafluoroethylene (PTFE, more popularly known as Teflon) (Lindstrom, Strynar, and Libelo 2011). On its own part, PFOS (which is usually used as a potassium or sodium salt) is main ingredient in *Scotchgard* and other similar stain repellents (V. L. Ochoa-Herrera 2008). It is also used in hydraulic fluids in commercial airliners (Lau et al. 2007).

Due to their surface tension lowering and wetting abilities, both PFOA and PFOS have historically been used in aqueous film forming foams (AFFFs) which are as the name suggests, used for firefighting (Knepper and Lange 2011; Merino et al. 2016; S. Park, Zenobio, and Lee 2018; Takagi et al. 2008; Gao and Chorover 2012; Hebert et al. 2002; Villagrasa, de Alda, and Barceló 2006; V. L. Ochoa-Herrera 2008). They have both also been used in household items such as non-stick cookware (Xiao, Simcik, and Gulliver 2013; Lau et al. 2007; Benford et al. 2008).

1.4 Occurrence

PFOA and PFOS have been detected in virtually every part of the world as well as in all manner of matrices- sediment, soil, seawater, groundwater and even drinking water (Benford et al. 2008; Key, Howell, and Criddle 1997; Vecitis et al. 2009; Skutlarek, Exner, and Farber 2006), which all makes it unsurprising that it has been detected in the serum of many human subjects. In Australia, Jack Thompson and coworkers (Thompson et al. 2011) detected 16 ng/L of PFOS and 9.7 ng/L, for PFOA as well as other shorter chain PFASs in surface waters. In China, Jin and coworkers found concentrations as high as 110.6 and 297.5 ng/L for PFOS and PFOA

respectively at sampling sites in the Yangtze River. PFASs were also found in Malaysia (Zainuddin et al. 2012.), Japan (Saito et al. 2004; Takagi et al. 2008; Taniyasu et al. 2003), South Africa (Mudumbi et al. 2014) and in the United States (Moody et al. 2003).

During the period 1960s-1990s, internal studies at DuPont showed the presence of PFOA in the blood of some of its workers. This data was however not reported to the authorities, which eventually led the company to pay a settlement fee to the US Environmental Protection Agency (EPA) in 2005 (Hogue 2005a).

1.5 Health Concerns/Toxicity

Various animal studies conducted over the past decade have shown various effects of PFASs. They were shown to affect the immune system in mice according to a 2008 study. In their 2009 paper, Peden-Adams and co-workers mentioned that the high levels of PFASs observed in wild animals were significant enough to “alter health parameters in people” (Peden-Adams et al. 2009). In 2003, the EPA started the process of conducting a full-scale assessment and review of PFAS’s to determine their risk level and to receive guidance on possible regulations. This came after the various instances where these compounds were detected in people who had occupational contact with them as well as members of the general populace. The results of this 10-year study were released in 2014 (Society 2005).

According to a 2012 story in Chemical and Engineering News (C&EN), “The C8 science panel (an independent research team) reports a connection between exposure to PFOA and high cholesterol” (Benford et al. 2008). In 2015, Chemours (a spin-off from Dupont) was ordered by a Federal U.S. jury to pay an Ohio woman \$1.6 million after she claimed that the PFOA used to

make Teflon was responsible for her kidney cancer (Reisch 2015). Similar personal injury suits against the company were expected to go to trial in 2017. In early 2017 however, Dupont and Chemours reached a settlement in 3,500 lawsuits and agreed to pay a total of \$670 million to people in Ohio and West Virginia who claimed injury due to PFOA (Reisch February 13, 2017)

PFASs have also been linked to pre-eclampsia in pregnant women (Stein, Savitz, and Dougan 2009) and attention deficit and hyperactivity disorder (ADHD) in children aged 12-14 (Hoffman et al. 2010).

1.6 Environmental Regulations

In 2005, an advisory board set up by the agency advised that PFOA be listed as a “Likely Human Carcinogen” and during the same year, a draft risk assessment was set for the entire group of compounds (Hogue 2005b; Eilperin 2005). In 2006, the EPA asked 8 chemical companies to voluntarily eliminate the production of PFASs at their facilities although it was unclear at the time how many of those companies intended to heed such request (Hogue 2006). In November that year, DuPont agreed to reduce the screening threshold near its West Virginia plant 300-fold, from 150,000 parts-per-trillion to 500 parts-per-trillion.

In 2009, the EPA set preliminary health advisory of 400 parts-per-trillion for PFOA and 200 parts-per-trillion for PFOS. In 2016 however, the agency finally set a lifetime advisory of 70 parts-per-trillion for any combination of PFOA and PFOS in drinking water (Morrison 2016b; Anonymous 2016).

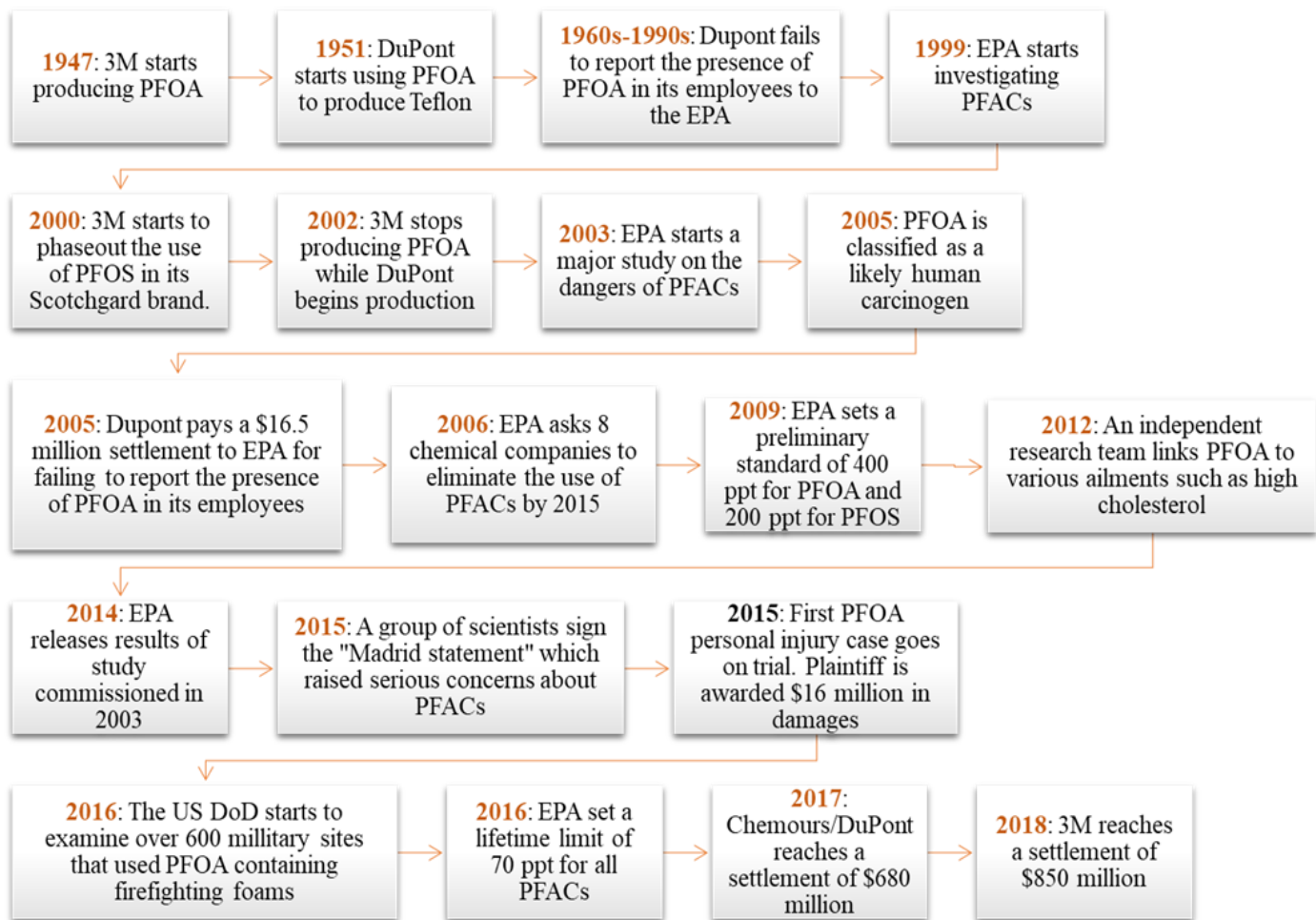


Figure 1.3 Timeline of PFASs in the United States (Morrison 2016a)

1.7 Analytical Techniques

Due to their unique physicochemical properties, PFOA and PFOS have presented analytical challenges in the past. Traditional high performance liquid chromatography (HPLC) is ineffective for the identification of PFASs because compounds like PFOS are generally not ultraviolet (UV) active (the mode of detection in traditional HPLC). This means that UV-Vis would also not be an effective method of analysis. According to literature, various methods based on liquid chromatography mass spectroscopy (LC-MS) have become among the most commonly used technique for analyzing PFASs. One of the major benefits of LC-MS is that PFASs can be routinely detected at ng/L levels and in addition, associated by-products or reaction intermediates (especially in cases of decomposition reactions) can potentially be identified simultaneously. One drawback of LC-MS is that the instrumentation is expensive and is highly sensitive to matrix interferences. HPLC with suppressed conductivity detection is another technique that has been employed with some success and is one that has some promise based on its relative low cost. Instrument manufacturers like Dionex (now part of ThermoFisher Scientific) and Metrohm have developed methods based on this technique that have shown detection limits in the ppb range. As mentioned earlier, this technique is significantly cheaper than LC-MS which makes it an attractive choice for laboratories without a lot of resources. However, given the EPA guidelines of 70 ppt for PFOA and PFOS, more work needs to be done to improve detection limits to that level in order to meet future regulatory demands.

Ochoa Herrera and co-workers have developed a method using Fluorine-NMR which is great for qualitative analysis but not as robust in terms of quantitation (V. L. Ochoa-Herrera 2008). A gas chromatography method has also been reported for the detection of PFASs.

Many of the techniques mentioned above often involve solid phase extraction (SPE) which serves as a mode of sample cleanup (to remove interferences) and/or as a sample pre-concentration step (to improve sensitivity).

Table 1.2 Analytical methods for the determination of PFASs in aqueous matrices

PFOA, PFOS or Both	Matrix	Sample volume (mL)	Extraction/cleanup	Analysis	LOQ/LOD	References
PFOA	Contaminated groundwater	55-200	SPE (SAX)	GC/EI-MS	36 µg/L	(Moody and Field 1999)
Both	Surface water	0.2-200	SPE (C ₁₈)	LC/(-)ESI-MS/MS	9-17 ng/L	(Moody et al. 2001)
Both	River water	40	SPE (C18)	LC/(-)ESI-MS/MS	10-50 ng/L	(K. Hansen et al. 2002)
Both	Wastewater	100	SPE (styrene divinylbenzene copolymer)	HPLC-Conductivity detection	50 µg/L	(Hori, Hayakawa, Yamashita et al. 2004)
PFOS	River water	1.0	Online extraction	LC/(-)APPI-MS	5.35 ng/L	(Takino, Daishima, and Nakahara 2003)
PFOA	Rainwater, surface water	500-1000	LLE	GC-MS	0.5ng/L	(Scott et al. 2006)
PFOA	Spiked water/modified diatomite	3	SPE (C18)	HPLC-Conductivity detection	N/A	(da Silva-Rackov et al. 2016)
Both	Spiked water	0.05	SPE (C18)	Fluorescence	46 ng/L	(Huang et al. 2016)
Both	Spiked water	0.025	N/A	UV (210 nm)	N/A	(Poboży et al. 2011)

1.8 Current Treatment Methods

Over the course of the past decade (at least), a lot of studies have been conducted and published on various techniques that have been developed for the treatment of PFASs in various matrices. Given the high stability of these compounds (as described in a previous section), it should be expected that many of such developed methods would face varying degrees of challenges.

Number of researchers Researchers such as Merino (and co-workers) (Merino et al. 2016) and Vecitis (and co-workers) (Vecitis et al. 2009) have published detailed review papers which have examined many of the various techniques that other researchers have developed for the treatment of PFASs. A look these studies as well as a few other individual studies suggest that treatment of PFASs at the moment involves any one of 3 major strategies- Physical treatment, Reductive decomposition and oxidation. Here is a summary of how they work.

Adsorption is probably the most popular physical treatment technique. Conceptually, it involves the accumulation of a substance at the surface of another (Çeçen and Aktas 2011). In this case the target compound (adsorbate) adheres onto the surface of the adsorbent (the thing that adsorbs) thus removing it from water and some of the more common examples in water treatment are granular activated carbon (GAC) and ion exchange resins (Çeçen and Aktas 2011; Knepper and Lange 2011). Ochoa-Herrera and Sierra-Alvarez demonstrated that PFOA and PFOS were effectively removed from spiked water samples. The same study also examined other materials such as sludge, silica, and zeolite with varying degrees of success (V. Ochoa-Herrera and Sierra-Alvarez 2008). Another study by Qiang Yu and co-workers (Yu et al. 2009) also found good removal of PFASs in water using GAC and ion exchange resins.

Another form of physical treatment for PFAS's is membrane filtration (Knepper and Lange 2011). For this application, the 2 more popular methods are nano-filtration (NF) which involves pore sizes of 0.00005-0.002 μm and reversed osmosis (RO) which involves pore sizes below 0.00005 μm (Knepper and Lange 2011). A 2006 study by Tang and Fu showed that RO was effective in removing PFOS from semiconductor wastewater (C. Y. Tang et al. 2006).

In general, physical methods such as membrane filtration, ion exchange and activated carbon treatment are effective methods for removing PFASs from water. The downside of these methods however is that none of them actually decomposes these compounds and this means that other steps such as incineration have to be taken which invariably leads to other concerns (Knepper and Lange 2011).

Table 1.3 Physical sorption of PFOA and PFOS from selected literature (Merino et al. 2016)

<i>Sorbent</i>	<i>Amount (g)</i>	<i>PFAS Concentration (mg/L)</i>	<i>Adsorption capacity</i>	<i>References</i>
Hematite	0.01-0.08	207	5.19	(Gao and Chorover 2012)
Multiwalled Carbon Nanotubes	0.001	0.1	406	(X. Li et al. 2011)
Electrocoagulation with Zinc	200cm ²	0.207	2,376	(Lin et al. 2015)
Hexagonal mesoporous silica (HMSc)	0.025	6.5	5.13	(Nassi et al. 2014)
Granular activated carbon	0.1	15-150	0.344	(V. Ochoa-Herrera and Sierra-Alvarez 2008)
Geothite	0.417	0.005-1	0.180	(Tang et al. 2010,)
Powdered activated carbon	0.48	50	520	(Yu et al. 2009)
Montmorillonite	0.1	0.6	0.108	(L. Zhao et al. 2014)
Kaolinite	0.1	0.6	0.104	(L. Zhao et al. 2014)

Reductive dehalogenation is a method that has often been used to treat sites contaminated with halogenated pollutants (Merino et al. 2016; Knepper and Lange 2011) and a few variations have been used for PFASs as well. Such reductive transformations often occur via attack by highly reactive nucleophiles. One such example is the hydrated electron (Merino et al. 2016). One reaction that produces hydrated electrons is the one between potassium iodide (KI) and UV light (254 nm). According to separate studies done by Park (H. Park et al. 2011, 1945-1953) and Qu (Qu et al. 2014; Qu et al. 2010), hydrated electrons generated from the reaction mentioned above attack and transform PFASs.

Another reaction of interest here is the UV-photolysis of isopropanol at high pH (> 12). This reaction results in the formation of a 2-hydroxyprop-2-yl radical which has led to the decomposition of PFOS (Knepper and Lange 2011). A study by Ochoa-Herrera and co-workers found that titanium citrate can react with the cobalt in vitamin B₁₂ to produce Co(I) which is a strong reducing agent (V. Ochoa-Herrera et al. 2008). At 70° C and pH 9, PFOA degrades to about 66% in 3 days (V. Ochoa-Herrera et al. 2008).

Under alkaline conditions, hydrogen peroxide and persulfate can produce superoxide radicals which are strong reducing agents. Separate studies by Da Silva-Rackov (and co-workers) (da Silva-Rackov et al. 2016) and Mitchell (and co-workers) (Mitchell et al. 2013) have both found PFOA to be decomposed in the presence of superoxide. Another study found that zerovalent iron (Fe⁰) nanoparticles coated with Mg-aminoclay degraded 38-96% of various PFASs in water (Arvaniti et al. 2015) although not much was known about the decomposition by-products of this process meaning that there is still some more work to do.

In summary, the degradation of PFASs through reduction pathways at this point requires a lot of work. Some of the studies that showed good reduction in PFAS concentrations lack adequate

information about potential decomposition byproducts and the studies that do show such information involve high energy processes that might be a challenge for real-world applications.

At this point, there is still a lot more work that needs to be done in this area.

Table 1.4 Reductive degradation of PFASs in selected literature (Merino et al. 2016) and (Trojanowicz et al. 2018)

<i>Catalyst</i>	<i>[PFAS] (mg/L)</i>	<i>Conditions</i>	<i>λ(nm)</i>	<i>Time (hrs)</i>	<i>Removal %</i>	<i>References</i>
Aminoclay coated nZVI	0.20	pH 3	N/A	0.33	40	(Arvaniti et al. 2015)
Fe(III)	0.1	20°C, pH 3.5, 34 g/L H ₂ O ₂	N/A	2.5	89	(Mitchell et al. 2013)
Ti(III)-citrate	30	70°C, pH 9.0, vitamin B12	N/A	168	90	(V. Ochoa-Herrera et al. 2008)
Aqueous iodide	8.28	pH 6.0–8.0	254	6	nd	(H. Park et al. 2009)
Fe-modified diatomite	10	0.3M PS/H ₂ O ₂ , pH 9	N/A	6	70	(da Silva-Rackov et al. 2016)
Aqueous iodide	10.35	740 mL, pH 9.0	254	6	9.39	(Qu et al. 2014)
Sodium sulfite	8.28	200 mL, pH 10.3	254	6	N/A	(Z. Song et al. 2013)
Dithionite	20	N/A	254/311	0-10	N/A	(Vellanki, Batchelor, and Abdel-Wahab 2013)
Aqueous iodide	8.28	40°C, pH 9, 0.15 g/L NaCl	254	6	nd	(C. Zhang et al. 2015)

In the field of environmental remediation, oxidation has always been a popular method of treating harmful contaminants. Of the many different oxidants used in water treatment, the hydroxyl radical $\text{OH}\cdot$ is among the most reactive (Knepper and Lange 2011). As a quick background, radicals (also known as free radicals) are reaction intermediates that are formed when a molecule/compound has an unpaired electron. Hydroxyl radicals are often produced via processes generally referred to as advanced oxidation processes (AOPs). The most commonly used AOP might be the Fenton reaction where hydrogen peroxide reacts with ferrous ions to produce the hydroxyl radical. Other AOPs involve UV based processes, and ozone-hydrogen peroxide processes (Brillas et al. 1998; Bautista et al. 2008; Rosenfeldt and Linden 2004; Knepper and Lange 2011).

Generally speaking, AOPs work via addition reactions to break carbon-carbon double bonds or by hydrogen abstraction (Knepper and Lange 2011). Unfortunately, due to the absence of either condition in PFASs, traditional AOPs are ineffective for their treatment (Pignatello, Oliveros, and MacKay 2006; Vecitis et al. 2009). Having said that, there are other methods based on oxidation that have proven to be successful for the decomposition of PFASs at certain conditions. First are sulfate radicals.

Sulfate radicals ($\text{SO}_4\cdot^-$) are produced either from the reduction of persulfate ion ($\text{S}_2\text{O}_8^{2-}$) or the peroxymonosulfate ion (HSO_5^-) by transition metal ions (Knepper and Lange 2011; Vecitis et al. 2009) and also by thermolysis of the former at temperatures greater than 40 degrees Celsius. They have also been used extensively in environmental remediation especially in the past 10-15 years (Nfodzo and Choi 2011b; Nfodzo and Choi 2011a; Liang and Lai 2008); (Vecitis et al. 2009; Hori et al. 2005; Lee et al. 2010).

Sulfate radicals are strong oxidants with reduction potentials in the range of 2.5-3.1 (Neta, Huie, and Ross 1988, Merino et al. 2016) and compared to hydroxyl radicals, they tend to react more selectively by way of electron transfer (Knepper and Lange 2011). A 2005 study by Hori and co-workers showed that 50 mM of persulfate (in the presence of UV light) was able to successfully decompose PFOA within 4 hours (Hori et al. 2005,) while another study by Lee and co-workers showed significant PFOS decomposition using persulfate activated by microwave heat and zerovalent iron particles.(Lee et al. 2010).

Direct UV photolysis is another oxidation technique used for decomposing PFASs. Photolysis is the process of using light energy to break down molecules and this is often dependent on the ability of the target compound to absorb light. In the absence of a catalyst, direct photolysis can only proceed if the photon energy of the light source is greater than the bond energies present in the target compound (Merino et al. 2016). At short wavelengths (<200 nm), PFOA can be broken down. This was demonstrated by Hori and co-workers by using a xenon-mercury lamp (Hori, Hayakawa, Einaga et al. 2004) vacuum UV (100-200 nm). Another study by Giri and coworkers (Giri et al. 2011) shows that C-F bonds were broken at 185 nm.

Photocatalysis is a method of using light energy to power a reaction with the aid of a catalyst and has been used for the decomposition of many organic contaminants (Merino et al. 2016) . Photocatalytic decomposition happens when light exposure produces an energy difference between the valence band and the conduction band of the catalyst. Titanium is one of the most common materials used for heterogeneous photocatalysis (Merino et al. 2016) and it is no surprise that it has been used for the decomposition of PFASs. One study by Ochiai and co-workers saw almost complete decomposition of PFOA in water after 4 hours (Ochiai, Moriyama et al. 2011) while a few other studies also saw good decomposition to varying degrees. Other

studies have used different semiconductor materials as heterogeneous catalysts for the treatment of PFASs. One study by Zhao and co-workers (B. Zhao 2011) used gallium oxide while Li and co-workers used indium oxide as a photocatalyst for PFASs decomposition.(X. Li et al. 2012).

Electrochemical oxidation is yet another method of destroying PFASs where they can either be destroyed by direct electron transfer from the anode (after being adsorbed) or in solution via strong oxidizing agents produced by electrolysis (Merino et al. 2016; Knepper and Lange 2011). The most commonly used material here are boron-doped diamond electrodes (BDDEs) and a number of researchers have successfully deployed them for the treatment of PFASs with varying degrees of success (Carter and Farrell 2008; Liao and Farrell 2009; Urriaga et al. 2015; Ochiai, Iizuka et al. 2011).

In summary, oxidative methods can be an effective way to treat PFASs. For many of them however, high energy methods such involving electricity, heat and light need to be employed which may make their application in the field quite challenging. More research is obviously needed in order to make these kinds of treatment more viable.

Table 1.5 Oxidative decomposition of PFASs from selected literature (Merino et al. 2016)

<i>Catalyst</i>	<i>[PFOA/PFOS] (mg/L)</i>	<i>Conditions</i>	<i>Wavelength (nm)</i>	<i>Time (hrs)</i>	<i>Removal %</i>	<i>References</i>
Fe-TiO ₂	25	250 mL, 14.2 Na ₂ SO ₄	254	12	69	(M. Chen et al. 2015)
Persulfate	25	25 °C, 1,000mL	254 & 185	2	92.6	(J. Chen and Zhang 2006)
TiO ₂ (P25)	1656	30 °C	315–400	9	32	(Gatto et al. 2015)
TiO ₂ (P25)	2070	30 °C	254	6	nd	(Ochiai, Moriyama et al. 2011)
TiO ₂ (RdH)	50	25 °C, pH 1.5–1.3, 7.5 g/L HClO ₄	254	7	86	(Panchangam et al. 2009)
β-Ga ₂ O ₃	0.5	25 °C, 150mL, pH 4.7	254	3	nd	(Shao et al. 2013)
TiO ₂ :MWCNT	30	23 °C, 250 mL, pH 2.0	365	8	nd	(C. Song et al. 2012)
UV-Fenton	8.28	200 mL, pH 3.0, 1.02 g/L H ₂ O ₂	254	5	98	(H. Tang et al. 2012)
Fe(III)	20	20–25 °C, 500 mL, pH 3.5–4.0	254	4	78.9	(Wang et al. 2008)
2-propanol (Alkaline)	20	T = 38–50 °C, 750mL	254	240	92	(Yamamoto et al. 2007)

nd= not determined

1.9 Nanomaterials and water treatment

Nanomaterials can be generally classified as having size in the range of 1-100 nm (Hornyak and others 2008; Williams and Adams 2006). In addition to the size limitation, the second thing that defines a true “nanomaterial” is that it must have properties that are different from larger sizes of the same material (Hornyak and others 2008; Williams and Adams 2006). For instance, rather than the characteristic “gold” color, gold nanoparticles are actually red in color. Nanomaterials tend to have larger surface areas and exhibit better reactivity than their microscale (bulk sized) counterparts. These properties lead to faster reaction rates, smaller quantities of materials required and more targeted reactions which are all desirable effects in environmental remediation (Hotze and Lowry 2010).

Materials at the nanoscale have the immense potential to vastly improve the efficiency of water treatment systems by improving quality and quantity of delivery all while being energy efficient (Williams and Adams 2006). One of the uses of nanomaterials in water treatment is for disinfection. A lot of metals can be used as disinfectants because they often present low cost and do not often lead to the formation of disinfection byproducts, unlike conventional disinfection processes (Hotze and Lowry 2010). In literature, there two major ways in which metallic nanomaterials engage in disinfection and these will be discussed in the next two paragraphs.

First, metals such as cobalt, copper, silver, and zinc, in small quantities, all work as disinfectants through a process known as the oligodynamic effect (Hotze and Lowry 2010, 138-164; Gladitz 2014). The oligodynamic effect is when metals (mostly heavy metals) act as a biocide and kill bacteria and viruses (Nägeli 1893). The source/reason behind this pathogen killing ability is not yet completely agreed upon in literature, but the hypothesis is that the metal ions deactivate thiol groups in enzymes which then affect the DNA of the bacteria and viruses (Hotze and Lowry

2010). Silver nanoparticles (AgNPs) have become the most widely used materials in this field as they have been found to attach to cell membrane surface; penetrate cell interior and react with materials therein; and alter permeability and respiration (Hotze and Lowry 2010). Another way in which nanomaterials can work as disinfectants is through photo-driven processes (Hotze and Lowry 2010) which have been described extensively in section 1.8.3 with titanium dioxide (TiO_2) nanoparticles being the most utilized here. Membrane treatment is another area that employs the use of nanomaterials (Hotze and Lowry 2010).

Zeolites can be impregnated into reverse osmosis membranes to create some kind of “molecular sieve” (Hotze and Lowry 2010). Silver nanoparticles can be embedded into membranes to prevent biofouling given their oligodynamic properties as mentioned earlier (Hotze and Lowry 2010). TiO_2 nanoparticles can also be impregnated into membranes and then use their photocatalytic properties to prevent fouling as well as to destroy unwanted contaminants (Hotze and Lowry 2010).

1.10 Nanoscale zerovalent Iron (nZVI)

Nanoscale zerovalent iron (nZVI) particles have over the years been used to treat various contaminants in water and one of the key factors that enable this process (especially on the large scale) is physical contact of the particles with the contaminant(s) (Hotze and Lowry 2010). Among the most important properties that determine nZVI particle reactivity are the chemical composition of the particles and the crystallinity (Hotze and Lowry 2010; Joo and Cheng 2006). The reactivity of nZVI particles because at the very large quantities required for environmental remediation, the costs can only be kept down if only a minimal amount is required (Hotze and Lowry 2010). In addition to reactivity, particle mobility and specificity are 2 other important considerations.

Freshly prepared/unreacted zerovalent tends to react quickly to become oxidized. This forms an often unreactive layer on the surface of the metal. This layer affects the overall reactivity of the nanoparticle because it limits the ability of iron to transfer electrons for reduction reactions. For this reasons, researchers have developed a number of methods for synthesizing nZVI particles with the aim of achieving optimal reactivity and stability (Hotze and Lowry 2010).

Nanoscale zerovalent iron (nZVI) have also become very useful for the treatment of a number of environmental contaminants primarily through reduction pathways (Liu, Majetich et al. 2005; Zhuang et al. 2011; Liu and Lowry 2006; W. Zhang, Wang, and Lien 1998; Dror, Moshe, and Berkowitz 2009; Lowry and Johnson 2004; Arvaniti et al. 2015). These nanoscale metallic particles typically have diameters in the range of 1–100 nm. In contrast to microscale zerovalent iron, nZVI particles are highly reactive due in part to their small size and high specific surface area, about 10–40 m²/g, compared to ~1 m²/g for the former (Wei et al. 2006; Lien and Zhang 2007). Another advantage with nZVI is that the particles can be more easily delivered into subsurface (for groundwater remediation) via direct injection.

Table 1.6 Properties of various nZVI particles synthesized by different methods (Hotze and Lowry 2010)

Particle synthesis method	Brief description	Particle Size (nm)	Surface Area (m²/g)	Crystallinity	References
Sputtering gas aggregation	Fe atoms are generated and then fired, argon gas is then used to slow them down and cause them to aggregate into nanoparticles.	2-100	N/A	Crystalline	(Baer et al. 2012)
Chemical reduction	Nanoparticles are produced by reacting solutions of iron salts with a strong reducing agent	30-40	36.5	Amorphous	(Liu, Choi et al. 2005)
H ₂ reduction	Reduction of goethite using hydrogen gas at high temperatures	70	29	Crystalline	(Toda 2011)
Precision Milling	Precision grinding of microscale feedstock using stainless steel beads	10-50	39.0	N/A	(S. Li, Yan, and Zhang 2009)
Green synthesis	Iron nanoparticle synthesis using green tea extracts	20-120	5.8	Amorphous	(Kuang et al. 2013)
Lithography grinding	Process involves breaking bulk materials down to nanoparticles	N/A	N/A	N/A	(Shan et al. 2009)

Table 1.7 Shows some of the common methods for synthesizing iron nanoparticles as found in literature. The physical properties of these particles are studied using instrumentation such as energy dispersive spectroscopy (EDS), electron energy-loss spectroscopy (EELS), transmission electron microscopy (TEM) and X-ray diffraction (XRD). EDS provides information on the chemical make-up of the sample and would show if any impurities are present. TEM beams electrons through the samples and is used for imaging and can also be used to estimate the particle size. XRD provides information about the crystal structure as well as other physical properties. It can also tell us if there are oxides on the particle surface, how much elemental iron is actually present and whether the particles are crystalline or amorphous. Reactive nanoscale iron particles (RNIP) which was commercially available from TODA Japan was synthesized using the hydrogen gas thermal reduction method reported in literature (Toda 2011; Hotze and Lowry 2010) and was shown to have a crystalline structure (Hotze and Lowry 2010).

Despite the fact that nZVI has proven to be quite effective for the removal of organic contaminants, some significant shortcomings do exist. Newly synthesized nZVI particles can be unstable, they are quite reactive the surface tends to get oxidized and “passivate” rather quickly and they often tend to agglomerate (Stefaniuk, Oleszczuk, and Ok 2016) thus reducing the operating surface area which in the first place is the one of the properties that makes them so attractive in the first place. For this reason, a number methods have been developed that modify nZVI particles and make them more effective for the treatment of organic contaminants (Stefaniuk, Oleszczuk, and Ok 2016; Hotze and Lowry 2010). Some of them are discussed in the following paragraphs. Doping metals like nZVI with noble metals such as palladium, platinum, silver, copper, nickel and rhodium, does improve the reactivity by enhancing the transfer of electrons to highly oxidized species (W. Zhang, Wang, and Lien 1998; Liu and Lowry 2006). Of

these, palladium has so far proven to be the most effective (Alonso, Beletskaya, and Yus 2002). The mechanics of this will be explained in the subsequent paragraphs.

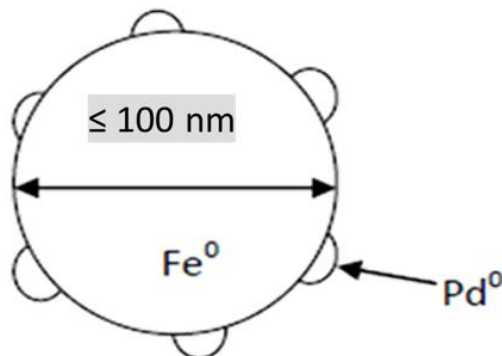


Figure 1.4 Schematic representation of palladium doped nanoscale iron

Nanoscale ZVI/Pd bimetallic particles are more reactive compared to non-palladized particles and the larger microscale particles. The presence of palladium facilitates a high surface reactivity which facilitates a more effective hydrodehalogenation process compared to ZVI and nZVI (W. Zhang, Wang, and Lien 1998; Liu and Lowry 2006). As such, the application nZVI/Pd particles might appear to be a promising technique for the reductive degradation of PFASs at ambient conditions.

The nZVI/Pd system is widely believed to occur because of 2 major factors. First is the catalytic activity at the palladium surface. Palladium adsorbs hydrogen gas produced via the electrolysis of water which then dissociates into atomic hydrogen as a formidable reducing agent (Lien and Zhang 2007; Wei et al. 2006). The second factor is the galvanic cell formed by the nZVI/Pd bimetallic system. Given that palladium is less active than iron, its presence on the iron surface creates galvanic cells with iron as the anode and palladium as the cathode (Wei et al. 2006; Lien and Zhang 2007). The electrons transferred from iron to palladium could then (theoretically) be

contributed to the fluorine atoms in PFOA to form fluoride ions. Reductive dehalogenation of organic compounds in the presence of metals are often surface-mediated reactions and typically involve either direct or indirect reduction or even both. The entire process occurs via diffusion of the reactant to the metal surface, a chemical reaction on the surface and then, the diffusion of the product(s) back into the solution. To overcome issues relating to mobility in porous media like the subsurface, nanoparticles are often coated on their surfaces to improve their performance (Hotze and Lowry 2010; Stefaniuk, Oleszczuk, and Ok 2016). Coating the particle surfaces in this manner helps to modify the surface charge and reduce agglomeration.

Because of the heightened interest in environmentally friendly materials, biopolymers such as starch, guar gum and carboxymethyl cellulose (CMC) are popular materials used in this application (Stefaniuk, Oleszczuk, and Ok 2016; Hotze and Lowry 2010). Emulsification is yet another way of modifying nZVI for the effective treatment of contaminated water (Hotze and Lowry 2010; Stefaniuk, Oleszczuk, and Ok 2016). In this case, the nZVI particles are placed in water and then covered in a oil layer. This helps make it easier for the particles to be transported into the subsurface for instance where they can better be in contact pollutant plumes.

Having nZVI particles embedded into support materials is another way to ameliorate some of the problems associated with the material. A commonly used material in this case is granular activated carbon (GAC). As reported widely by Choi and coworkers (Choi, Agarwal, and Al-Abed 2008; Choi, Al-Abed, and Agarwal 2009a; Choi, Al-Abed, and Agarwal 2009b; Choi and Al-Abed 2009), nZVI can be synthesized in-situ in the pores of GAC using the sodium borohydride method and using these materials, they were quite successful for the treatment of PCBs (polychlorinated biphenyls). One of the major advantages of this kind of material is that it has the ability to concentrate the contaminant and make it a bit easier to treat. Also, in many

cases, by-products can also be sorbed onto the support material which is a good thing especially when some of the by-products are more hazardous than the parent material.

1.11 Objectives of this study

At this point, nZVI/Pd appears to be the most promising technique working at ambient conditions for the reductive dehalogenation of PFASs. Although defluorination might be more difficult than dechlorination because C–F bonds (particularly, C(sp³)–F bond) are stronger than C–Cl bonds, few studies utilizing either ZVI, nZVI or nZVI/Pd, to the best of our knowledge, have reported the capability. It is hard to assume there have been no research activities on the issue. It is speculated that results showing successful defluorination of PFASs have not been observed in spite of significant effort. Presumably, (i) no or negligible decomposition of PFASs is observed on ZVI materials, (ii) defluorination of PFASs, if any, cannot be explained by the known ZVI chemistry, or (iii) removal of PFASs, if any, can be ascribed to other mechanisms such as adsorption and complexation rather than reductive defluorination.

As a result, in an attempt to answer the question on the reactivity of ZVI materials with PFASs, this study is aimed at examining whether or not nZVI/Pd, in comparison to ZVI and nZVI, can remove PFOA as a probe PFAS in water and if so, to also determine the mechanistic driving force behind the process.

CHAPTER 2

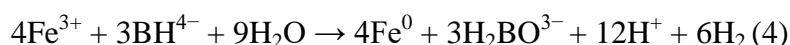
Methodology

2.1 Chemicals and reagents

Perfluorooctanoic acid, sodium borohydride, sodium hydroxide, sulfuric acid and boric acid was purchased from Aldrich (St. Louis, MO). Reactive Nanoscale Iron Particles (RNIP) was from Toda Kogyo (Japan), HPLC grade acetonitrile was obtained from Acros (New Jersey) and ultra-pure water was produced by a Milli-Q filtration system (Millipore; Billerica, MA).

2.2 Preparation of nanoscale ZVI/Pd particles.

Rather than prepare the nanoparticles from iron salts, we started with commercially available RNIP supplied by a vendor. The manufacturers of the RNIP powder prepared the particles with an iron oxide coating, which was intended to keep the particles stable and to allow for slow reactivity (which is useful for in-situ remediation applications). To make the RNIP more reactive, we reduced the iron oxide layer by employing the widely used sodium borohydride reduction method illustrated in equation (4) below (Lien and Zhang 2007, 110-116).



To reduce 1 gram of RNIP, the powder was weighed and added to a beaker containing 12.5 mL of a 30% methanol solution to form a slurry. Then, 1.25 grams of sodium borohydride is weighed and dissolved in 5 mL of water. Once this was added, the solution started to bubble and as soon as all of the sodium borohydride had completely dissolved, this solution was added dropwise to the RNIP slurry. It was important to do this part slowly because the process yields hydrogen gas which could lead to explosions.

After all of the sodium borohydride had been added, the whole setup was allowed to sit till the bubbling stopped (at least 90 minutes) and then it was filtered, after which the particles were thoroughly rinsed with methanol to get rid of any unreacted borohydride.

For palladium doping, 6 mg of palladium acetate was weighed and then dissolved in 10 mL of methanol. This solution was shaken repeatedly until the palladium salt had completely dissolved. The reduced iron particles were then immersed in the palladium acetate solution and then shaken using a rotary shaker until the characteristic color of palladium acetate had turned colorless indicating palladium reduction. After the doping procedure had been completed, the particles were again filtered and rinsed with methanol. Afterwards, the particles were stored in methanol in an air-tight container until they were ready for use.

The palladium loading for most of the experiments in this study was 0.67% (of nZVI) except in cases where we examined the effects of palladium during which the concentration varied.

2.3 Batch reaction procedures

All reactions were carried out in a 100 mL batch reactor starting with PFOA concentration of 20 mg/L (0.048 mM) prepared from a stock solution. After the reactor was set up, pH was tested and adjusted if necessary. 3 mL samples of each reactor were collected and a buffer was added to keep the pH at 7. This sample represents the initial concentration (C_0). The reaction began as soon as the iron was added, pH was read and samples were collected at 5, 10, 15, 30, 60, 120 and 180 minutes. The amounts of nZVI/Pd used for this study ranged from 1 g/L to 20g/L. Each sample was filtered using a 0.45 μ m syringe filter and briefly vortexed.

Most reactions were conducted without pH adjustment but for those reactions that required that we evaluate the effects of pH on the degradation of PFOA, H_2SO_4 and NaOH were added to

adjust the initial pH as needed. Reactors containing no added iron particles served as the control. At the same time, experiments were also performed with microscale ZVI and nZVI (without palladium) both at 5 g/L.

2.4 Sample cleanup (solid phase extraction)

Potential interferences from the collected samples were removed by solid phase extraction techniques. For PFOA analyses, the vacuum manifold was loaded with Agilent BondElut C18 cartridges (100mg, 3ml). The cartridges were conditioned by eluting 2 mL of methanol and then rinsed/equilibrated with 2 mL deionized water with care taken not to allow the cartridges to dry up (and lose efficiency).

Next, 2 mL of the sample (previously collected from the reactor) was injected onto the cartridge and passed through at a flow rate of about 1 mL/min. This relatively slow flow rate was necessary to ensure that the target compound (in this case, PFOA) was completely adsorbed onto the cartridge. After loading the sample, the cartridge is rinsed (to remove any impurities that could interfere with analysis) with 2 mL water and then finally, PFOA is eluted from the sample matrix using 1 mL of methanol at a rate of 1 ml/min. This helps to concentrate the samples and make them easier to analyze.

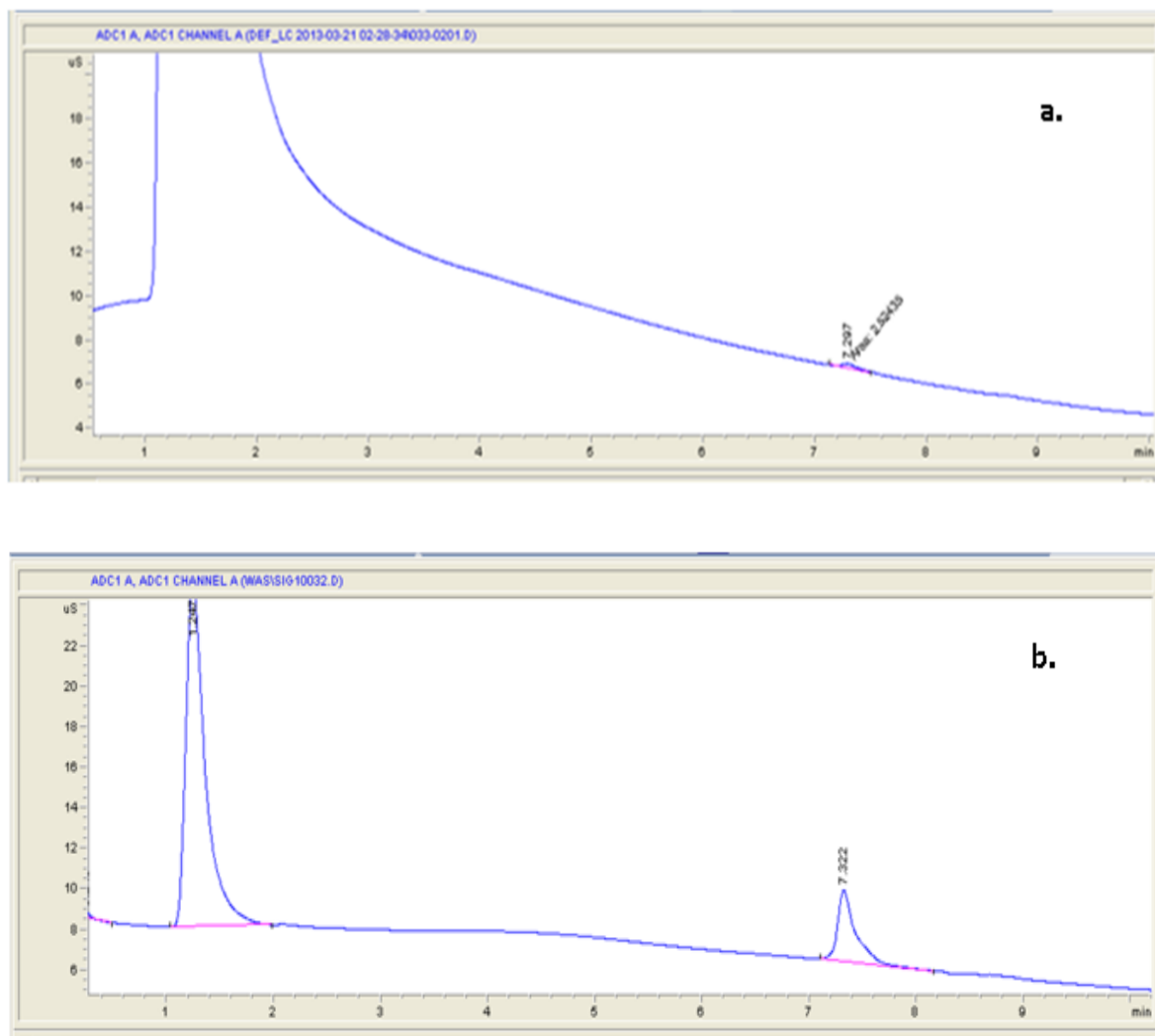


Figure 2.1 HPLC Chromatogram of PFOA, (a.) without SPE, (b.) with SPE.

A similar procedure was used for fluoride analysis but this time using an Agilent BondElut SCX cation exchange cartridges (100mg, 3ml) were used (to eliminate iron). Similar to PFOA analysis, the cartridges were conditioned by eluting 2 mL of methanol and then rinsed/equilibrated with 2 mL deionized water. 2 mL of the sample was injected onto the cartridge and the eluent was collected for fluoride analysis. After the SPE procedure, the eluted samples are collected into 8 mL culture tubes and then transferred into 2 ml HPLC vials for analysis.

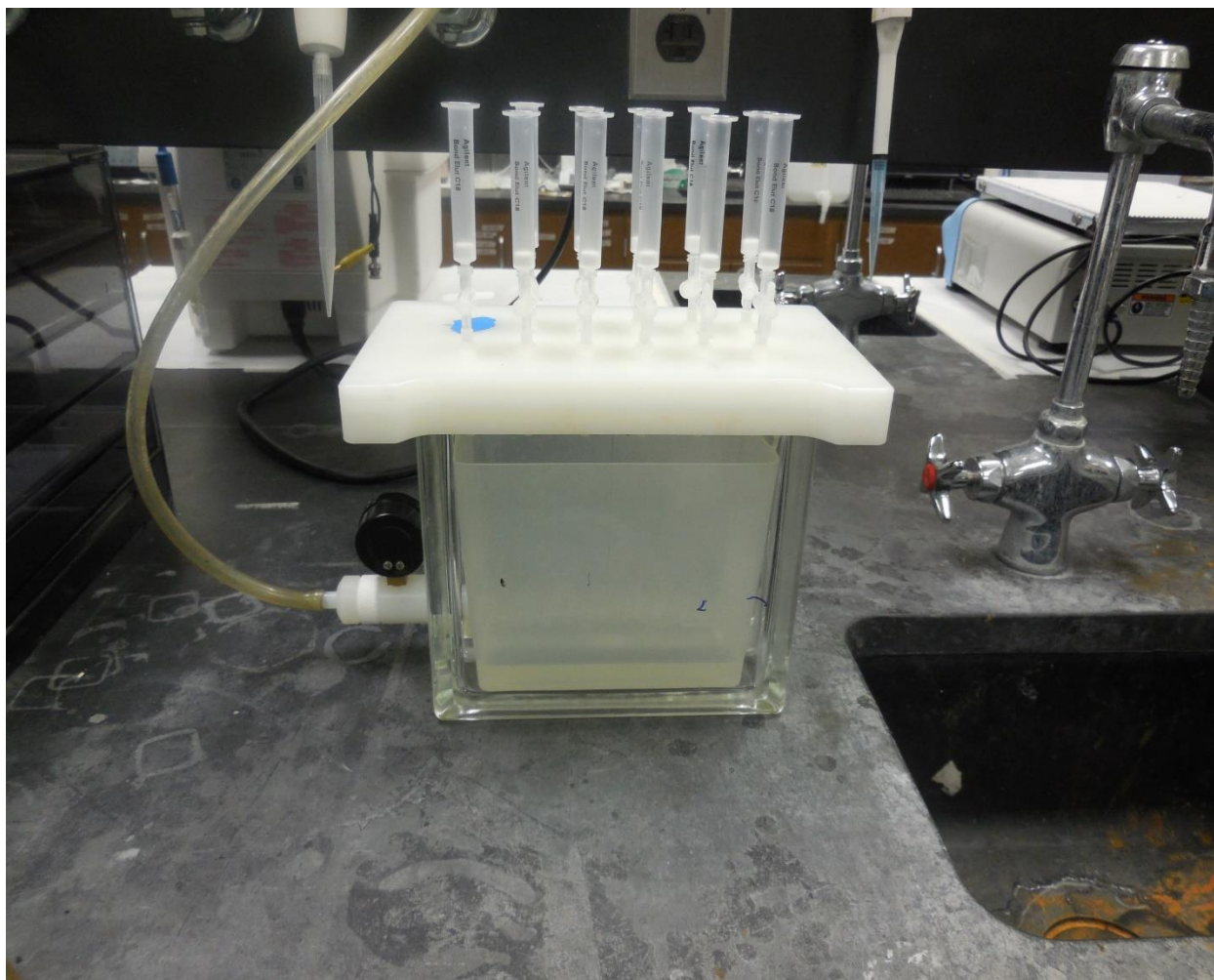


Figure 2.2 SPE Apparatus

2.5 HPLC Analyses

PFOA was analyzed using a high-performance liquid chromatography which included a quaternary pump and the separation was performed on an Acclaim PA2 guard cartridge and column (both DIONEX/Thermo Fisher) while ion suppression was done by an The signal from a conductivity detector (Shimadzu Scientific) was transmitted to the Chemstation software for processing by an Sample elution was done via a gradient flow of water, acetonitrile and a solution of 9 mM NaOH and 100 mM H₃BO₃ over a period of 12 minutes.

To monitor the disappearance of PFASs in water, HPLC with suppressed conductivity was employed according to methods developed by Subramanian and co-workers. Typically, the system involves an HPLC unit and a conductivity detector all connected together. In this lab however, what was available was an Agilent 1200 series HPLC for which the manufacturer does not produce a conductivity detector. The solution was to use a detector (Shimadzu CDD-10AVP) from another manufacturer (Shimadzu Scientific) and then the signal from this was transmitted to Agilent's Chemstation Software using an Agilent 35900E A/D interface (Agilent Technologies).

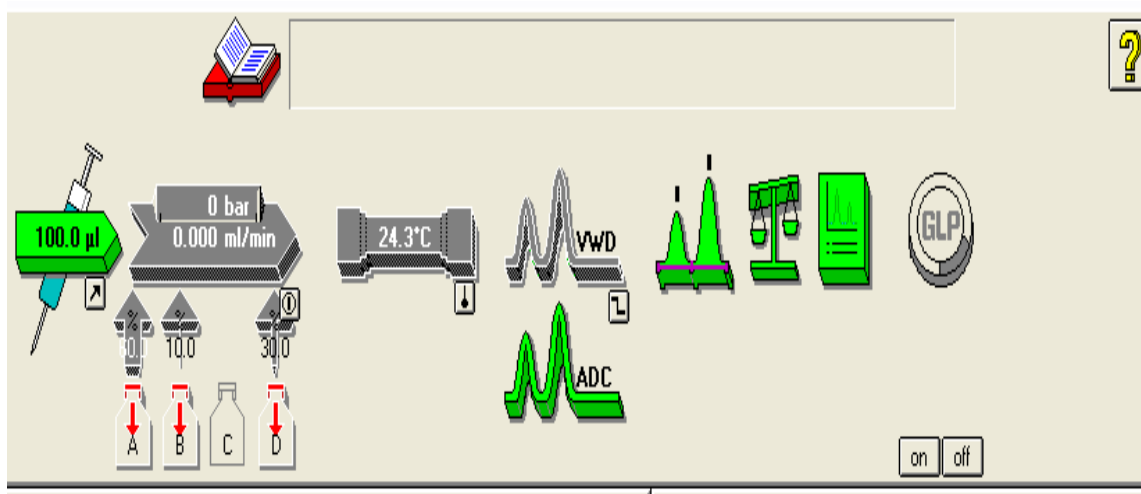


Figure 2.3 Flow diagram of the HPLC process from the Chemstation software

The mobile phase comprised of deionized milli-q water (A), acetonitrile (B) and a solution of 9 mM NaOH and 100 mM H₃BO₃ (Boric Acid) (D). The stationary phase was a Bonna Agela Venusil AQ C18 column with a particle size of 3 µm, diameter of 4.6 mm and length of 450 mm. The background conductivity of the bromate buffer was diminished using a Thermo Scientific AMMS-300 Anion MicroMembrane suppressor (DIONEX/Thermo Fisher). The suppressor was

regenerated by running 10 mN sulfuric through its membranes using nitrogen flow at a rate of 3 mL/min.

Table 2.1 Gradient program for PFOA identification by HPLC with suppressed conductivity detection.

Time (Minutes)	A%	B%	D%	Flow rate (mL/min)
0	60	10	30	1.4
7.5	15	55	30	1.4
10	15	55	30	1.4
10.9	60	10	30	1.4

As illustrated in Table 2.1, the gradient elution started with 10 % acetonitrile which was ramped up to 55% in 7 minutes, held at 55% till 10 minutes and then brought back down to 10% at 10.9 minutes. The analysis was stopped at 12 minutes and the equilibration time (before the next sample) was 2 minutes. The injection volume was 100 μ L while the column and conductivity oven temperatures were both set to 30⁰ C. The conductivity signal was set to 100 μ s/volt while the data collected at intervals of 10 Hz.

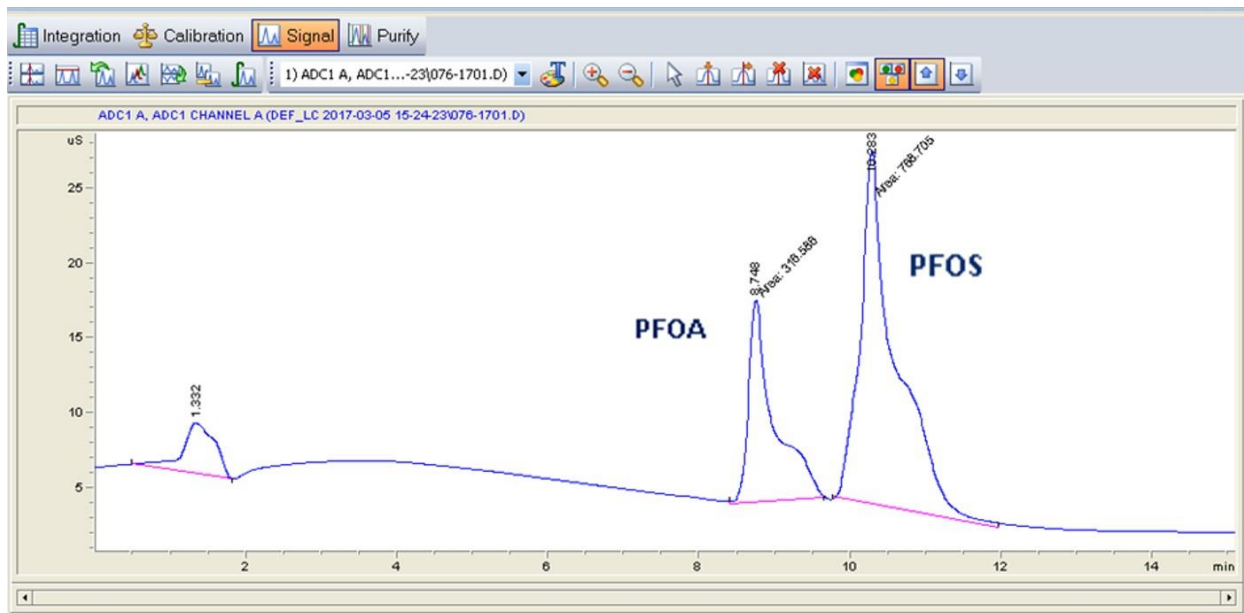


Figure 2.4 Flow diagram of the HPLC process from the Chemstation software

PFOA was found to elute at around 9 minutes while PFOS eluted at 10 minutes as illustrated in figure 2.4 above. Blank samples and various QC standards were run at frequent intervals to ensure that the system was working as intended.

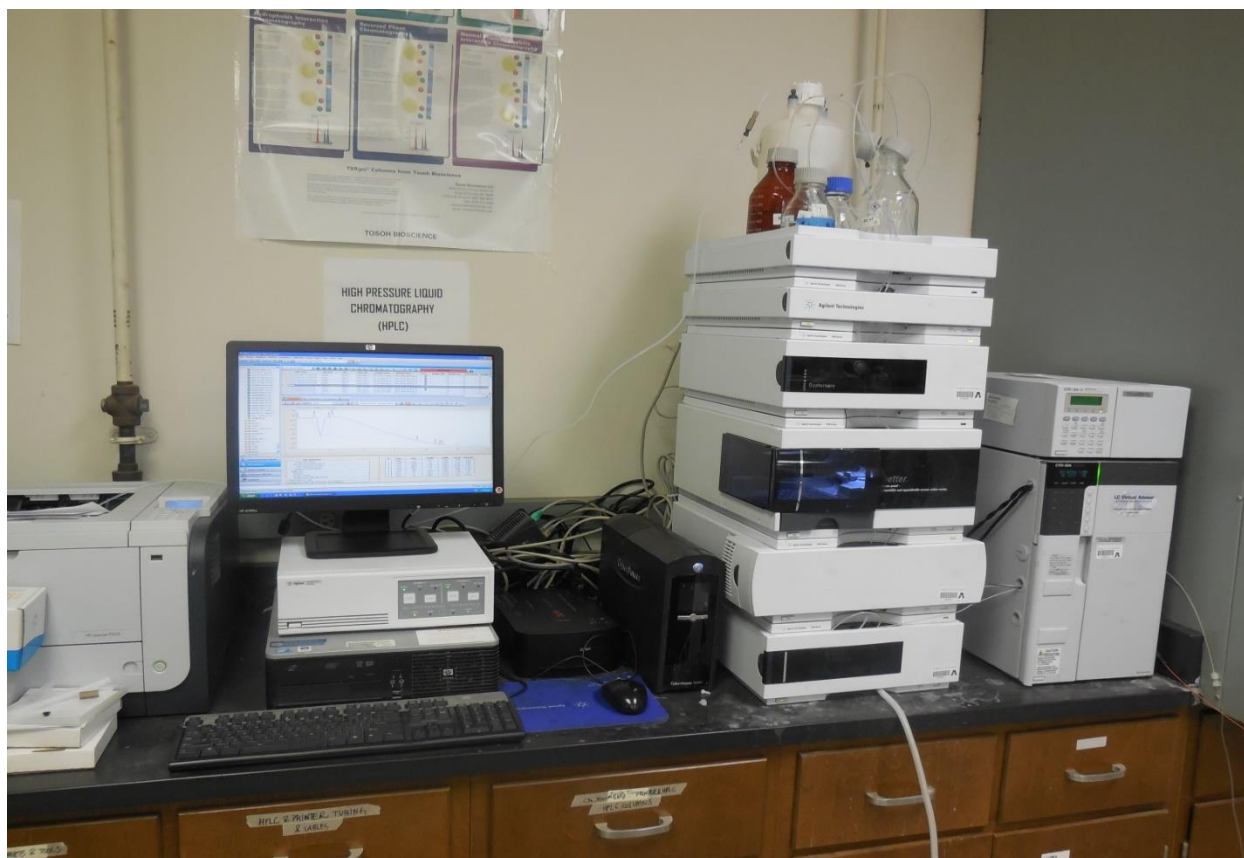


Figure 2.5 HPLC- Conductivity Detection Setup

2.6 Ion chromatography analysis

Potentially released fluoride ions were measured using ion chromatography. The instrument used for this study was a Dionex DX 10000 LC with a quaternary pump and a conductivity detector. For this analysis, the mobile phase was a mixture of 4.5 mM of sodium carbonate and 0.8 mM of sodium bicarbonate while the stationary phase was a Dionex Ionpac AS14A column (4 mm × 250 mm) which was immediately preceded by a Dionex Ionpac AG14A column (4 mm × 50 mm). The high background conductivity of the mobile phase was eliminated using a 4 mm Dionex AERS suppressor which was regenerated using the recycled mobile phase outflow from

the conductivity detector and operated at a current of 25 mA. The data for each run was collected at intervals of 5 Hz



Figure 2.6 Ion chromatography setup

As was the case with HPLC, blank samples and various QC standards were run at frequent intervals to ensure that the system was working as intended.

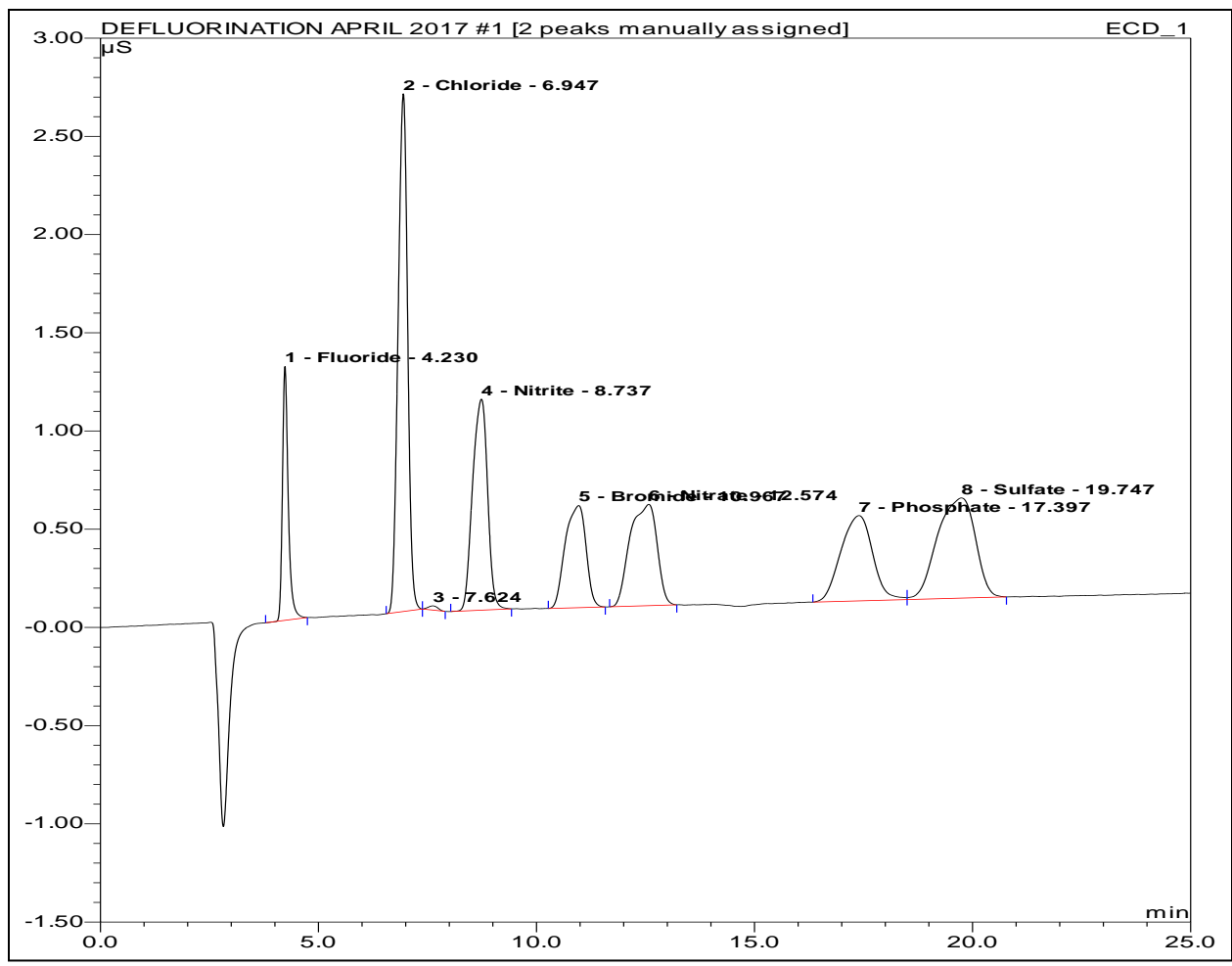


Figure 2.7 Ion Chromatogram of 7 common anion standards

2.7 Total organic carbon measurements

PFOA and any possible reaction by-products in solution were determined as Total Organic Carbon (TOC) using a Shimadzu TOC-V_{CSH} analyzer (Japan). Total organic carbon itself was indirectly measured using the TC - TIC method. In other words, total carbon (TC) and inorganic carbon (TIC) for each were measured individually and then the difference represents the TOC given that $TOC + TIC = TC$. TIC was calibrated using a mixture of carbonate and bicarbonate

and the samples were analyzed by acidifying the samples and then measuring the resultant carbon dioxide using the instrument's in-built nondispersive infrared (NDIR) detector. TC was calibrated using potassium hydrogen phthalate standards ranging from 0.3 mg/L – 10 mg/L and then was measured by thermal oxidation (at 680 °C) followed by determination of the resultant carbon dioxide by NDIR.

Samples from the reactor were collected and vacuum filtered through a 0.45 µm Whatman filter. All blanks, standards and unknown samples were acidified with HCl before analysis.



Figure 2.8 Total organic carbon instrument

2.8 LC-MS/MS measurements

Possible decomposition products of PFOA were measured using liquid chromatography with triple quadrupole mass spectrometry (LC-MS/MS).

The analysis was performed on a Shimadzu LCMS-8040 instrument and the multiple reaction monitoring mode (MRM) was used to identify and quantify PFOA and any other products formed during the reactions. Separation was performed with an Agilent XDB-C18 column (50 mm × 4.6 mm, 1.8 μm particle size) with the column temperature set at 30 °C. The flow rate was 0.1 mL/min and the mobile phase was 10 mmol/L ammonium acetate (A) and methanol (B).

The target compounds were eluted under a gradient as follows 10–20% B for 2–3 min, 20–50% B for 3–5 min and 50–70% B for 4–5 min. Then held for 4 minutes and then back down to 10% for 4 minutes. MS detection was operated in the negative electrospray ionization (ESI) mode.



Figure 2.9 LC-MS/MS instrumentation

2.9 Zeta potential analysis

The size and Zeta potential nZVI and nZVI/Pd particles in water were measured under different pH conditions. A Horiba SZ-100 instrument (Figure 2.10) using dynamic light scattering (DLS) and laser Doppler electrophoresis (LDE) for particle size and Zeta potential analysis respectively, was applied. DLS is commonly used and has proven to be very effective for measuring the size of particles when they are dispersed in suspension (Wu and Choi 2016). The method used in this study for the zeta potential and particle size analysis was adapted from the one developed by Wu and Choi (Wu and Choi 2016) Based on light scattering of the nZVI particles, their hydrodynamic diameter is calculated by using the Stoke-Einstein equation Particle size was measured at the 173° detection angle for 2 minutes (Wu and Choi 2016). Zeta potential is calculated from mobility by using the Smoluchowski model (Wu and Choi 2016).



Figure 2.10 Zeta potential/particle size analyzer

Prior to analysis on the zeta-sizer, the particles were dispersed using a Misonix S-4000 Sonicator. Nanoscale ZVI particles were dispersed in water at a fixed concentration of 50 mg/l. Based on previous studies from this lab, sonication was programmed at probe energy intensity of 60 W and sonication for 3 minutes followed by quiescence for 1 minute and after 2-3 repetitions, the samples were sent to the zeta-sizer for analysis.



Figure 2.11 High power sonicator

2.10 Physical characterization of iron particles

ZVI and nZVI particles were characterized using various methods to determine their physicochemical properties. To determine the visual morphology of the iron particles, a JEM-2010F (JEOL) high-resolution transmission electron microscope was used while a Kristalloflex D500 diffractometer (Siemens) was used to study the X-ray diffraction of the particles.

2.11 Calculations

The TOC removal efficiency was calculated Eq. (6) as follows:

$$\text{TOC removal (\%)} = (C_0 - C_t) / C_t \times 100 \quad (6)$$

Where C_0 is the TOC before the reaction and C_t is the TOC of the solution at any given time t (minutes).

The defluorination efficiency for each sample was calculated based on the following equation.

$$\text{Defluorination (\%)} = CF^- / (0.688 \times C_0) \quad (7)$$

C_0 was the initial concentration of PFOA; and CF^- was the concentration of the F^- at any given time. 0.668 represents the ratio between the molecular weight of all fluorine atoms in PFOA ($15 \times 19 \text{ g/mol} = 285 \text{ g/mol}$) and the total molecular weight of PFOA.

CHAPTER 3

Results

3.1 Physical properties of nZVI particles

Since many previous studies have already characterized the same ZVI materials, brief effort was given to simply identify the presence of zerovalent Fe and nanoscaling of particles, as shown in Figure 4.1 (Choi et al. 2009; Choi et al. 2008; Liu and Lowry 2006; Liu et al. 2005a; Liu et al. 2005b).

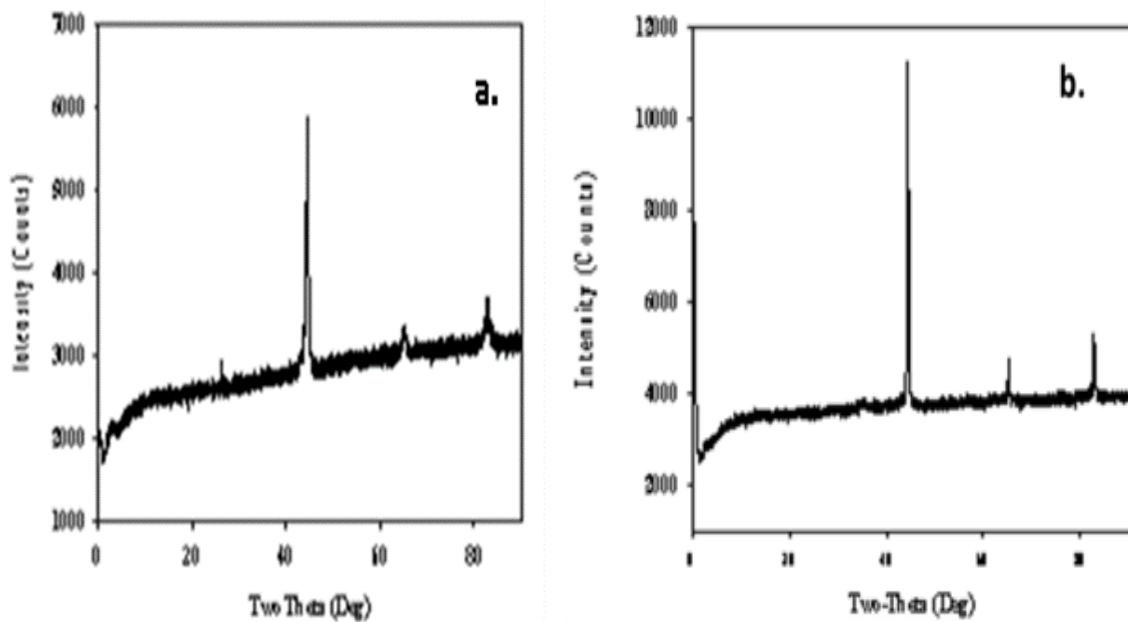


Figure 3.1 X-ray diffraction patterns of (a) nanoscale ZVI (b) microscale ZVI.

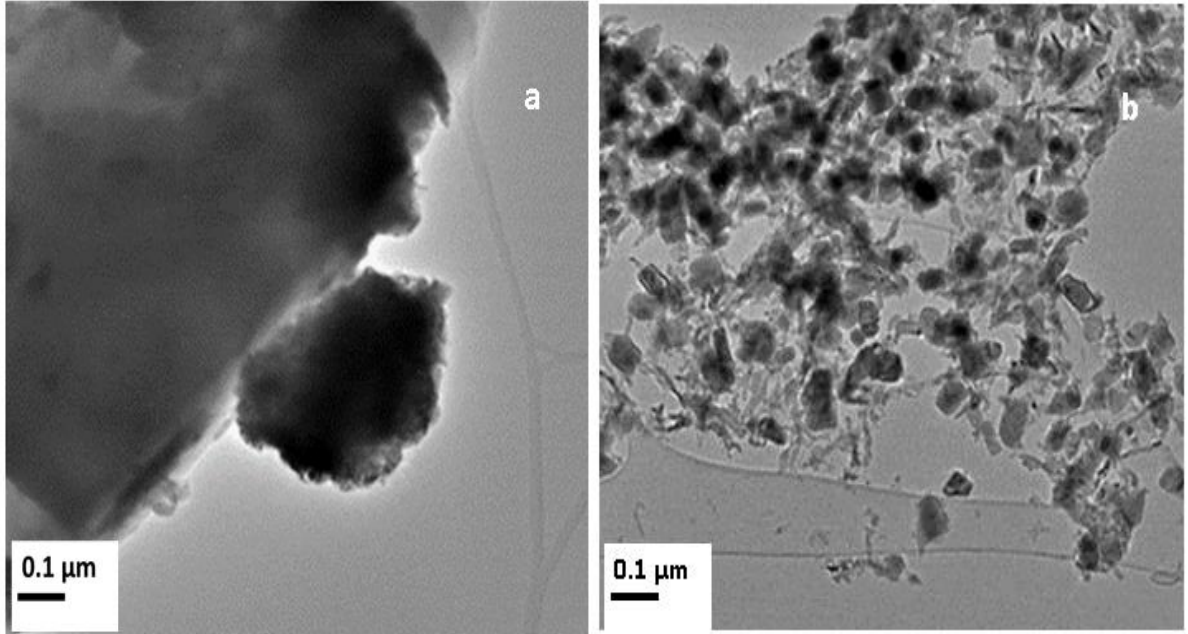


Figure 3.2 High-resolution transmission electron microscopic images of (a) microscale ZVI. (b) nanoscale ZVI

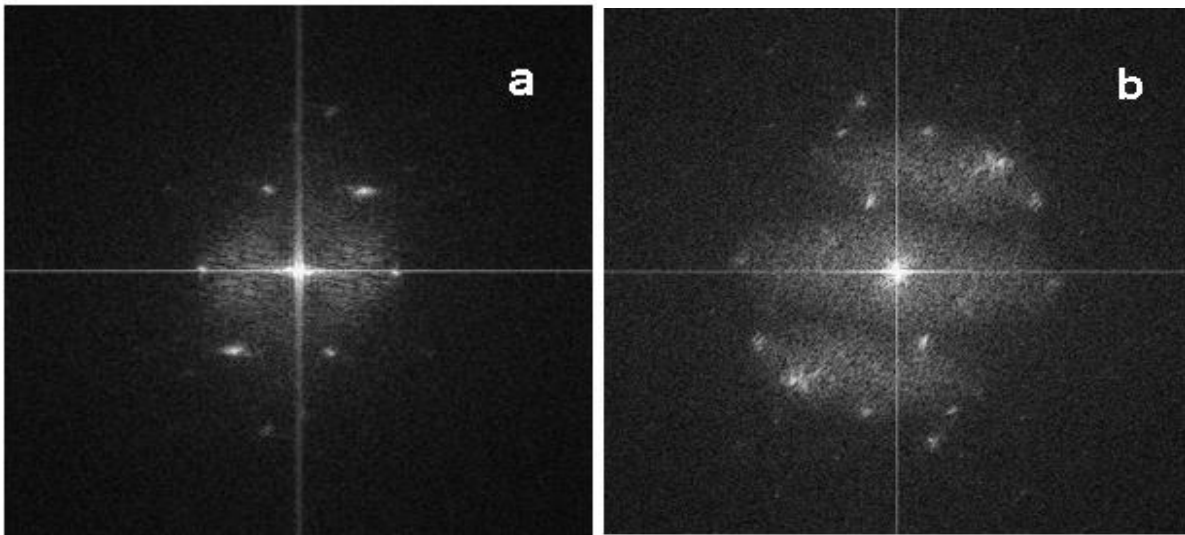


Figure 3.3 Fast Fourier Transform (FFT) diffraction pattern for a. microscale ZVI and b. nanoscale ZVI

The size of nZVI shown in Figure 3.2 (b) was ranged to 35-100 nm and averaged at around 45 nm. Their hydrodynamic diameter measured by a particle size analyzer was around 70 nm.

Surface area of nZVI was 30 m²/g according to the supplier. The microscale ZVI particles in Figure 3.2 (a) are obviously of a much larger size. ZVI materials used in this study were believed to exhibit the similar reactivity to those reported previously. The XRD pattern shown in Figure 3.1 (b) indicated that nZVI was crystalline rather than amorphous and the characteristic peak at 2θ of 45° indicated that nZVI was predominantly made of Fe in zerovalent state (Liu et al. 2005b). Doping of nZVI with such a small amount of Pd did not significantly change the overall properties of nZVI (Choi et al. 2009; Choi et al. 2008).

3.2 Comparison of ZVI Materials

Figure 3.4 shows the reactivity of ZVI materials with PFOA. As expected, control test without ZVI showed no removal of PFOA. ZVI (micron-size ZVI) showed negligible removal of PFOA while nZVI showed significant removal of PFOA most probably due to its higher surface area. As easily expected from the known reactivity of nZVI/Pd superior to nZVI, nZVI/Pd exhibited the highest removal of PFOA.

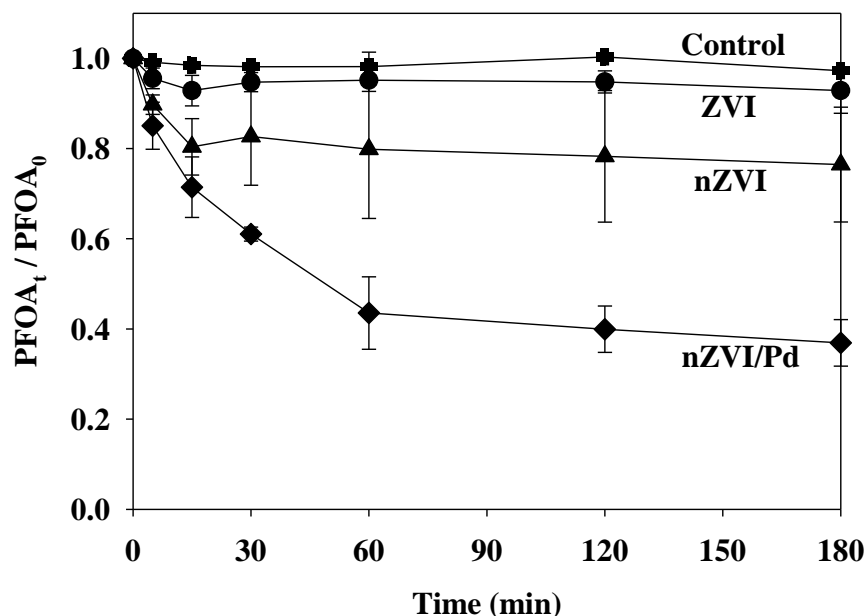


Figure 3.4 Effect of various ZVI particles on PFOA removal (20 mg/L PFOA, 5 g/L ZVI materials, and pH 5)

Interestingly, however, PFOA removal did not continue after initial significant removal within 15 min and 60 min in both cases of nZVI and even nZVI/Pd, respectively. The reactivity of ZVI materials might have been quickly exhausted. But this explanation does not seem realistic because high dose of ZVI materials at 5 g/L was used and particularly nZVI/Pd was reported to continuously decompose halogenated chemicals within the time frame (Choi et al. 2009; Liu et al. 2005b). More plausible explanation to the PFOA removal trend might be adsorption of PFOA to ZVI materials with limited sorption capacity, rather than chemical reaction, i.e., defluorination. Although exact mechanisms are not clear at this moment, it was found that doping of nZVI with Pd is in favor of PFOA removal via either defluorination and/or adsorption (will be discussed later). It should also be noted Pd as its ionic form Pd^{2+} , once dissolved in

water during the reaction, was completely reduced and deposited back onto nZVI surface (Eq. 5), while keeping Pd content in nZVI constant at 0.67%. The quick transformation of Pd²⁺ to Pd⁰ was confirmed by colorless solution at all times (i.e., orange color if Pd²⁺ is present).

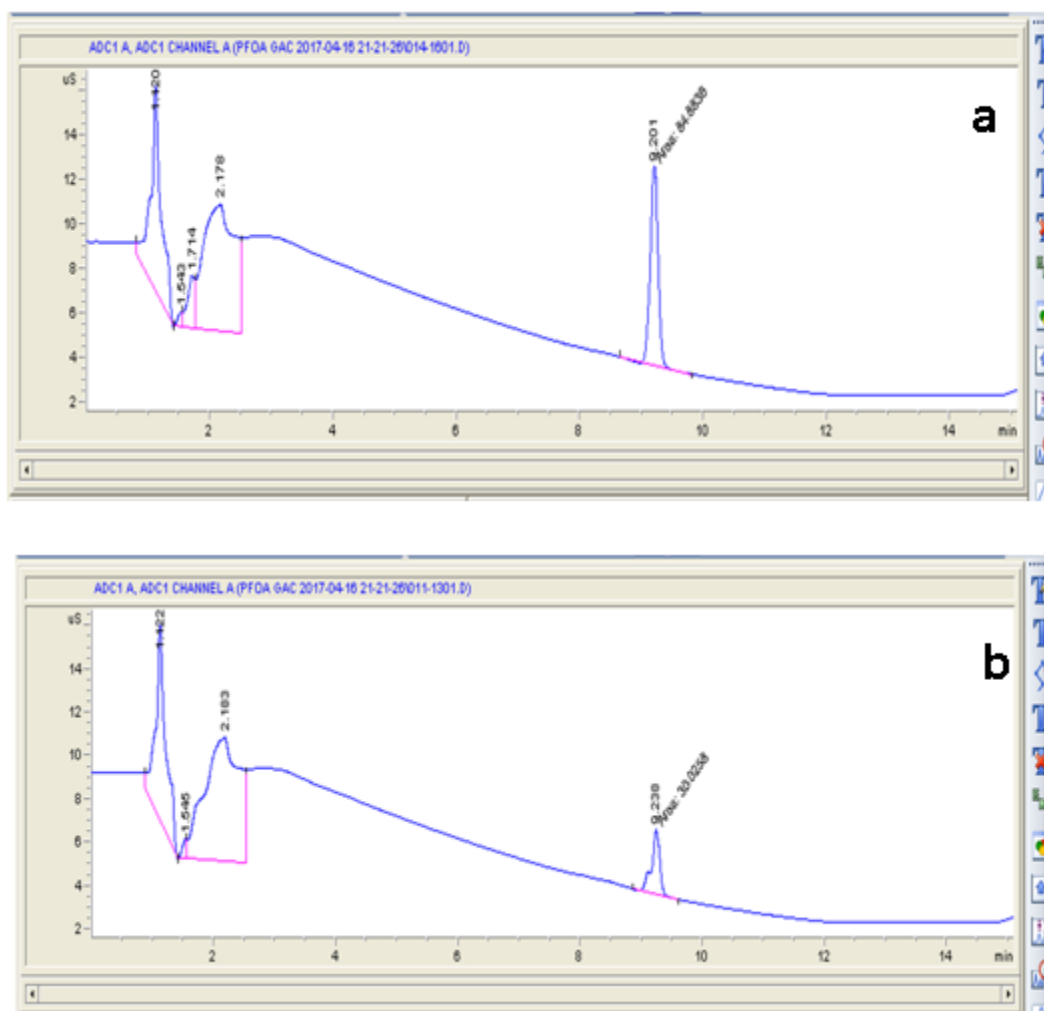


Figure 3.5 0-minute (control) sample (a.) and 3-hour sample (b.) of 5 g/L nZVI/Pd. 20 mg/L PFOA

3.2 Effects of Reaction pH, nZVI/Pd Dose, and PFOA Concentration

Since nZVI/Pd showed the highest removal of PFOA, more studies employing nZVI/Pd were performed to find best removal options for PFOA and also to explain PFOA removal

mechanisms. Figure 3.6 shows PFOA removal at various initial pH conditions at 3-11. No buffer was used to avoid analytical interference for PFOA and reaction of nZVI/Pd with buffer species. Reaction pH at initial 3 and 5 increased to around 7, right after nZVI/Pd addition and then pH change was not significant over time, while other initial pH cases showed negligible pH change. Acidic pH conditions, in particular pH 3 followed by pH 5, obviously demonstrated faster PFOA removal (details will also be discussed later).

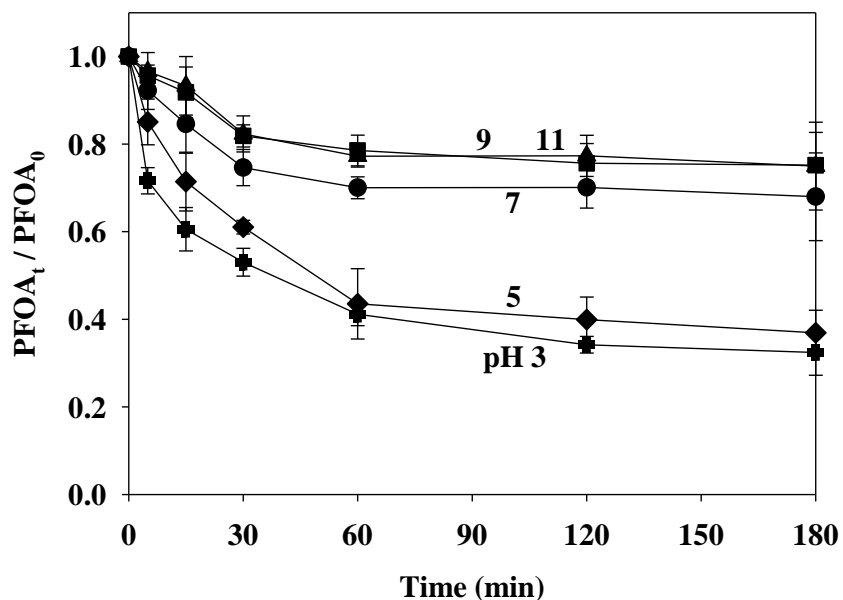


Figure 3.6 PFOA removal at various initial pHs (20 mg/L PFOA and 5 g/L nZVI/Pd).

Figure 3.7 shows the effect of concentration of nZVI/Pd at 1-20 g/L on removal of PFOA. As expected, higher doses of nZVI/Pd removed more PFOA. The rate of PFOA removal seemed to increase with increase of nZVI dose.

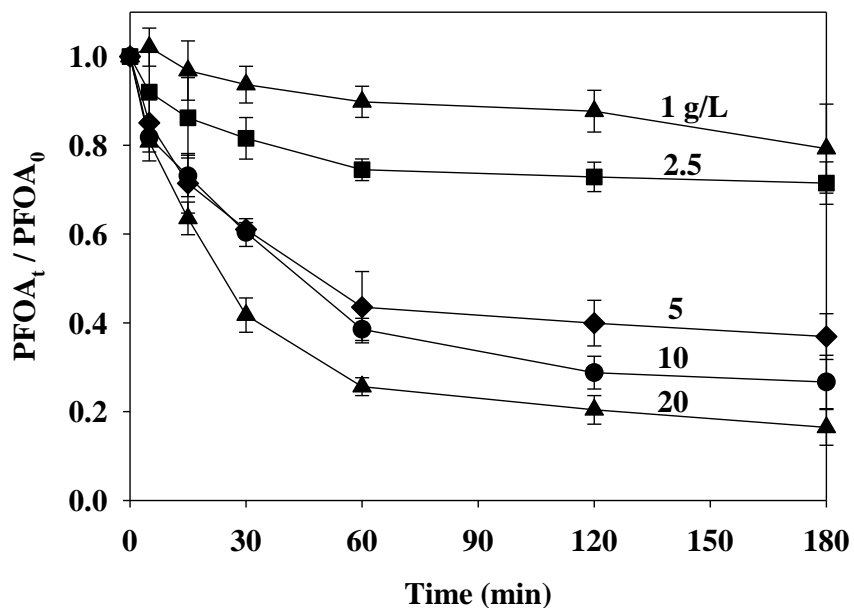


Figure 3.7 PFOA removal at various nZVI/Pd concentrations (20 mg/L PFOA and pH 5)

Figure 3.8 shows the effect of concentration of PFOA at 5-80 mg/L on its removal. As expected, cases tested with higher initial PFOA concentrations showed more PFOA removal with respect to total mass of PFOA removed. Unexpectedly, however, higher initial PFOA concentrations were ended up with higher removal efficiency, e.g., 32% for 5 mg/L vs. 92% for 80 mg/L. Final concentrations of PFOA after 180 min were very similar at 6-8 mg/L regardless of initial PFOA concentrations ranging 10-80 mg/L (except for 5 mg/L).

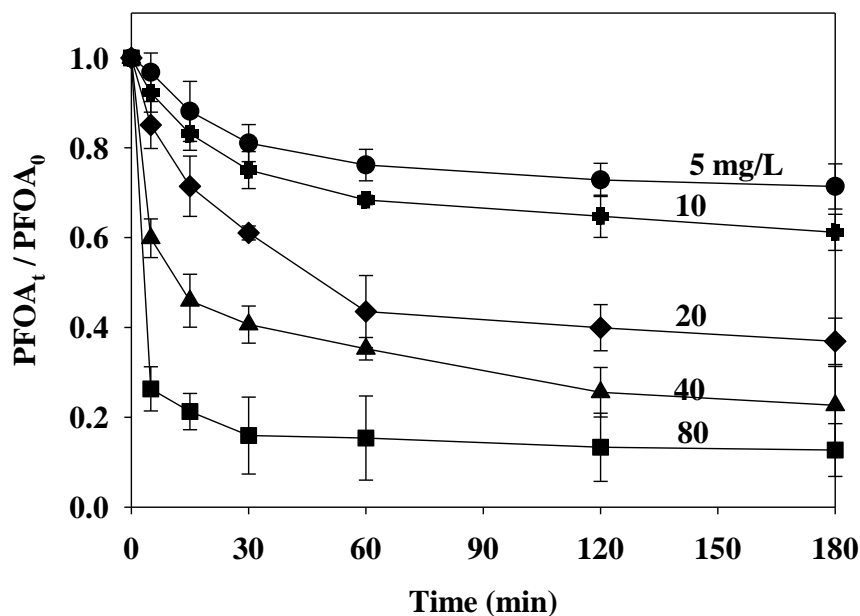


Figure 3.8 PFOA removal at various PFOA concentrations (5 g/L nZVI/Pd and pH 5)

The most interesting finding from the results in Figures 3.4, 3.6 and 3.7 was the PFOA removal trend. Regardless of initial pH conditions, nZVI/Pd doses, and PFOA concentrations, the removal trend was very similar to that discussed in Figure 3.4, i.e., initial fast removal and then negligible (or much slow) removal, cautiously implying adsorption than reaction as possible PFOA removal mechanism.

3.3 Results on TOC, MS/MS, and Fluoride

In an attempt to find mechanisms for the observed PFOA removal on nZVI/Pd (i.e., known chemical reactions such as defluorination vs. other mechanisms such as adsorption), TOC removal, reaction intermediates identification, and fluoride ion detection were examined.

Figure 3.9 shows TOC removal in the aqueous phase containing PFOA. Among ZVI materials, nZVI/Pd showed highest TOC removal, followed by nZVI and ZVI. If chemical reactions really occur to decompose organic chemicals, decrease in aqueous TOC is directly due to mineralization of organic chemicals (i.e., PFOA and, if any, reaction intermediates) completely into H₂O, CO₂, and many other simple inorganic species. In this case, TOC removal should be substantially slower than PFOA removal or disappearance in water, as typically observed (Eskandarian et al. 2016).

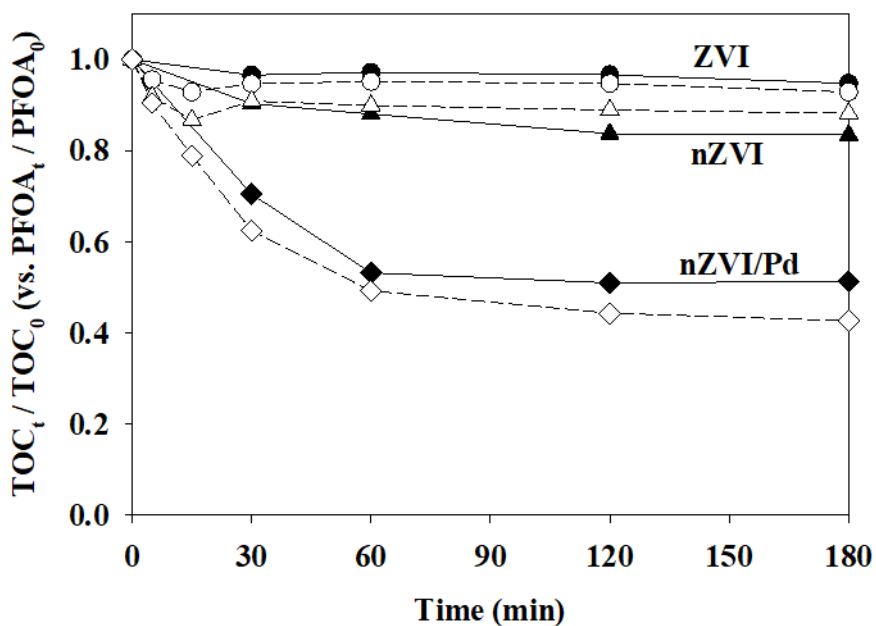


Figure 3.9 Effect of various ZVI particles on TOC removal (20 mg/L PFOA, 5 g/L ZVI materials, and pH 5).

In Figure 3.9, TOC removal is compared with PFOA removal, which is extracted from Figure 3.4 and expressed with empty dots with dashed lines. Meanwhile, if adsorption occurs, decrease in aqueous TOC is simply due to mass transport of PFOA from water to solid ZVI materials. In

this case, TOC removal in water should be theoretically the same as PFOA removal in water. In comparison between TOC removal in Figure 3.9 and PFOA removal in Figure 3.4, TOC removal kinetics were very similar to PFOA removal kinetics, and there was no significant retardation. PFOA removal on nZVI/Pd was slightly or marginally faster than TOC removal within 10% difference. The result indicates adsorption was dominant than chemical reaction for PFOA removal. However, the result is also possible for a case in which both adsorption and reaction occur at nZVI/Pd surface and reaction intermediates stay at the surface as adsorbed.

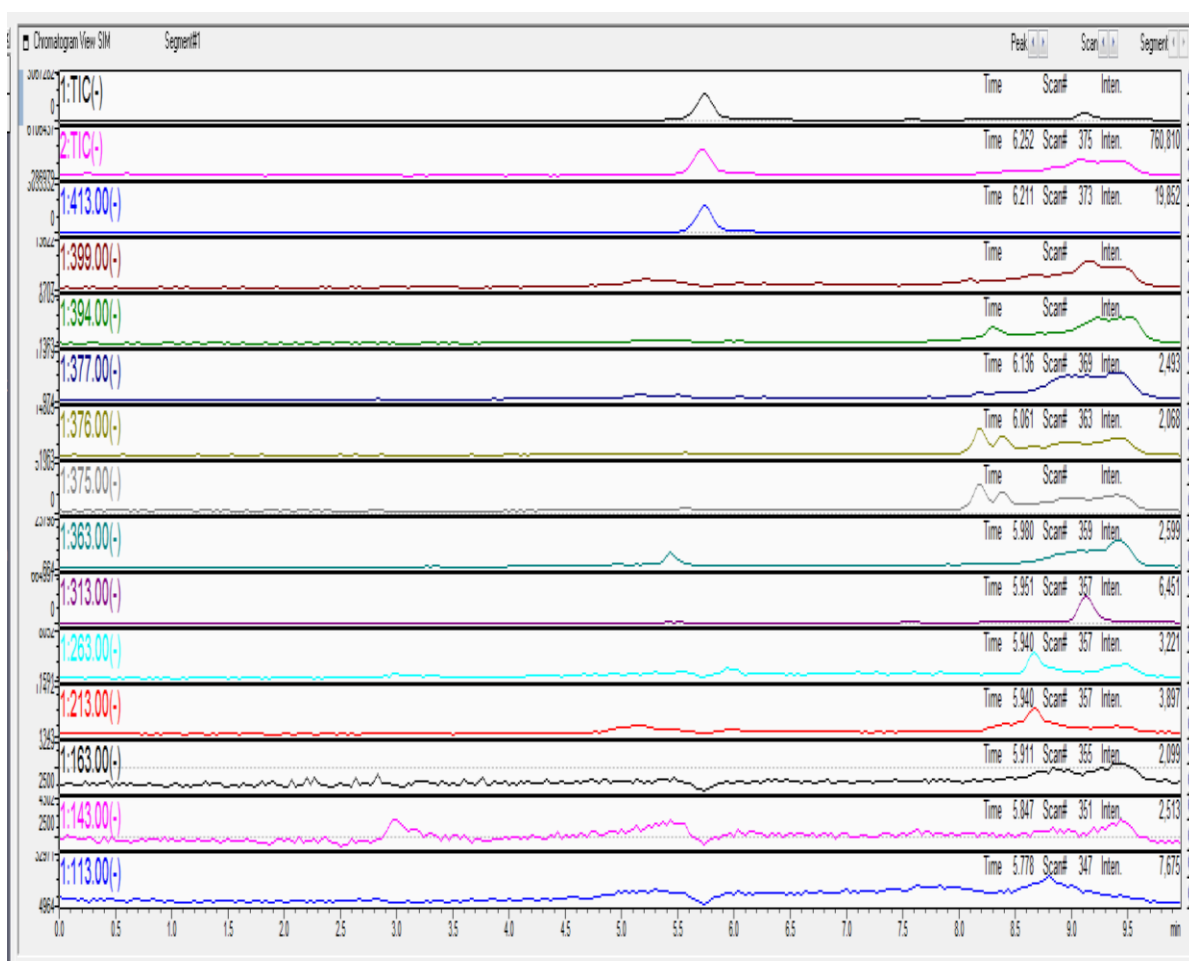
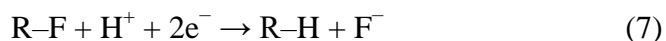


Figure 3.10 LC-MS/MS of PFOA reactor sample

To identify any reaction intermediates produced by any chemical reactions if occurring (mostly reductive defluorination), cations and anions in some aqueous samples were scanned through LC-MS/MS. In anion scan, only one noticeable peak at mass to charge ratio of 413 was observed, which is for PFOA. Cation scan showed some peaks, which were, however, very similar to those from control samples without PFOA. No meaningful peaks were also observed for the extracts from nZVI/Pd solid. Lastly, detection of fluoride ions in water was performed because defluorination of PFOA by nZVI/Pd might have released fluoride ions as shown in Eqs. (6) and (7). However, fluoride ion concentration in water did not change much in spite of significant TOC removal shown in Figure 3.10. All the results on TOC, MS/MS, and fluoride supported that the observed PFOA removal was not closely associated with reaction (i.e., defluorination) but interestingly with possibly adsorption.



3.4 PFOA Removal Kinetics and Mechanisms

It seems there was no significant chemical transformation of PFOA even in the presence of nZVI/pd. To further explain the observed PFOA removal and obtain insight on the physicochemical process occurring at nZVI/Pd surface interacting with PFOA, kinetic models and adsorption isotherm models were employed. Figure 3.11 shows the amount of PFOA adsorbed onto nZVI/Pd, which was calculated from the result in Figure 3.9 showing PFOA removal in the aqueous phase, assuming that there was no chemical transformation of PFOA. Dissolution of nZVI/Pd into water was not significant under initial pH 5 condition (less than 0.4%), keeping the nZVI/Pd solid content unchanged.

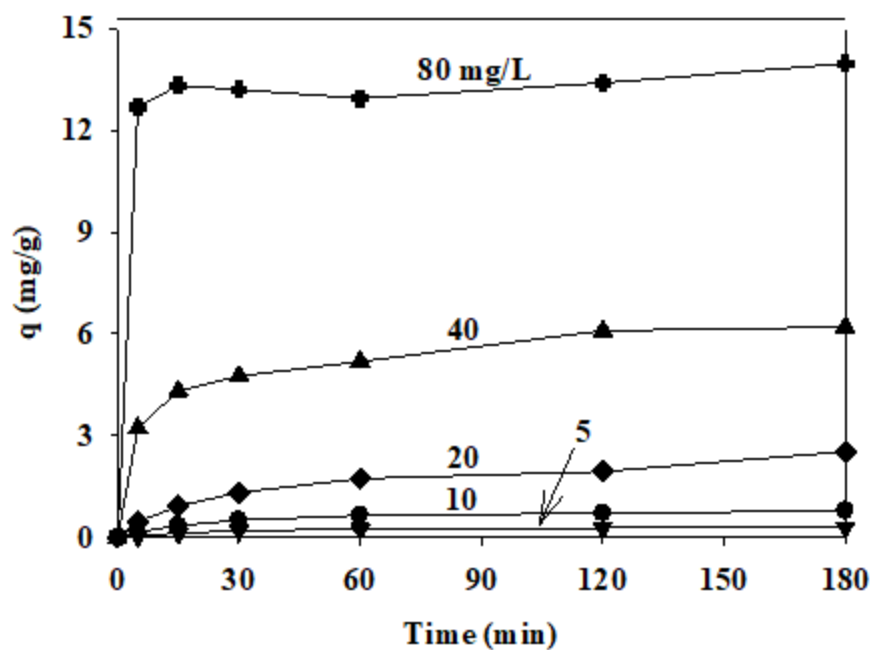


Figure 3.11 Adsorption of PFOA onto nZVI/Pd at various PFOA concentrations (5 g/L nZVI/Pd and pH 5)

As expected, higher solid phase PFOA concentrations were observed in cases of higher initial PFOA concentrations in water. To study adsorption kinetics, pseudo first-order model was compared with pseudo-second-order model (L. Zhao et al. 2014; Qu et al. 2009) as shown in Eqs. (8) and (9), respectively, where q_t and q_e (mg/g) are the amounts of PFOA adsorbed onto nZVI/Pd surface at time t (min) and at equilibrium, k_1 (1/min) and k_2 (g/mg/min) are pseudo-first and second order adsorption rate constants, and v_0 (mg/g/min) is initial adsorption rate. Plotting graphs of $\log(q_e - q_t)$ versus t for pseudo first order and t/q_t versus t for pseudo-second order showed a linear relationship between the associated parameters. Table 3.1 summarizes the rate constants and calculated q_e values.

Table 3.1. Comparison of Rate Constants and Calculated q_e Values of the Kinetic Models at Various Initial Concentrations of PFOA (5 g/L nZVI/Pd and pH 5)

Initial PFOA concentration (mg/L)	$q_{e, \text{obs}}$ (mg/g)	Pseudo first order			Pseudo-second order		
		$q_{e, \text{calc}}$ (mg/g)	k_1 (1/min)	R^2	$q_{e, \text{calc}}$ (mg/g)	k_2 (g/mg/min)	R^2
5	0.29	0.23	0.0242	0.980	0.34	0.0881	0.983
10	0.78	0.55	0.0184	0.943	0.58	0.0505	0.967
20	2.52	1.55	0.0187	0.964	2.37	0.0182	0.999
40	6.20	3.17	0.0191	0.977	6.64	0.0149	0.996
80	13.97	3.63	0.0223	0.816	13.8	0.0328	0.999

Based on the regression coefficient (R^2) greater than 0.967 in all cases, PFOA adsorption seemed to follow pseudo-second-order kinetics and q_e calculated from the pseudo-second-order kinetic model was very close to q_e observed. Yu and coworkers (Yu et al. 2009) reported that the pseudo-second-order model assumes that sorption process is dominated by chemisorption where chemical interactions are possibly involved.

$$\log(q_e - q_t) = \log q_e - \frac{k_1}{2.303} t \quad (8)$$

$$\frac{t}{q_t} = \frac{1}{k_2 q_e^2} + \frac{t}{q_e} = \frac{1}{v_0} + \frac{t}{q_e} \quad (9)$$

An isotherm curve correlating aqueous phase PFOA concentration (C_e , mg/L) and solid phase PFOA concentration (q_e , mg/g) at equilibrium was plotted, as shown in Figure 3.13.

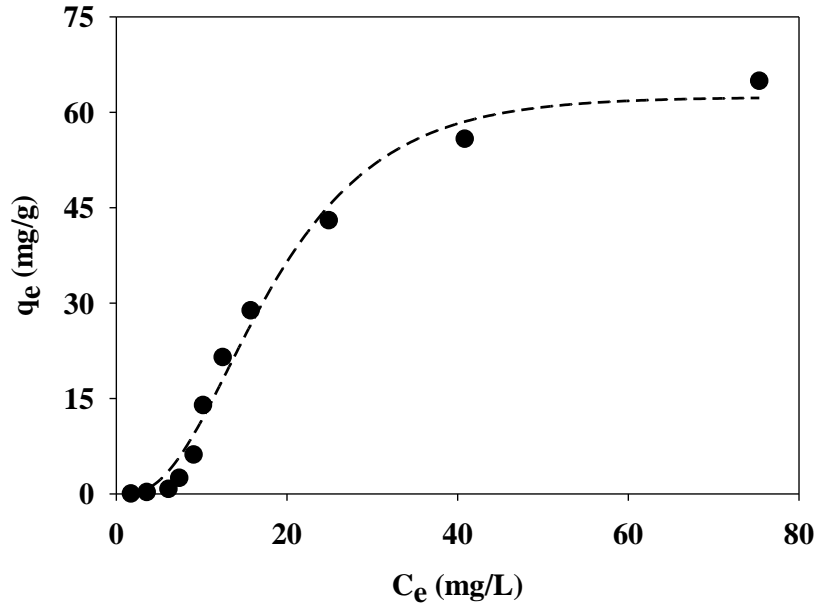


Figure 3.12 Isotherm of PFOA adsorption onto nZVI/Pd (dots: experimental data and curve: Chapman isotherm model).

For the isotherm determination, additional experiments with other initial PFOA concentrations than those used in Figures 3.8 and 3.11 were conducted, resulting in total 11 pairs of C_e and q_e .

At first look, the isotherm did not follow general models such as Langmuir and Freundlich, as shown in Eqs. (10) and (11), respectively, where Q_0 (mg/g) is maximum adsorption capacity, b (L/mg) is Langmuir adsorption constant, and k_F and n are Freundlich constants. Rather, Chapman isotherm model shown in Eq. (12), where k and c are Chapman constants, was best fitted with the isotherm data at R^2 of 0.983. Chapman constants were 0.0993 for k and 3.6429 for c .

$$q_e = \frac{b Q_0 C_e}{1 + b C_e} \quad (10)$$

$$q_e = k_F C_e^n \quad (11)$$

$$q_e = Q_0 (1 - e^{-k C_e})^c \quad (12)$$

Table 3.2. Calculated isotherm constants for the Freundlich, Langmuir and Chapman isotherms

Isotherms	Parameters
Langmuir	$k_L=0.0127$
	$Q = 141.73$
	$R^2= 0.9126$
Freundlich	$k_f=2.6131$
	$1/n=0.7714$
	$R^2= 0.8762$
Chapman	$Q= 62.37$
	$k= 0.0993$
	$c=3.6429$
	$R^2= 0.9825$

In order to interpret the unique S-shaped isotherm, explain the superior adsorption capability of nZVI/Pd to nZVI, and thus infer the mechanism for the observed PFOA adsorption onto nZVI/Pd, we looked into possible interaction of nZVI/Pd with PFOA reported in previous studies. (Arvaniti et al. 2015) pointed out that the surface charge of nZVI is important for determining the removal efficiencies of PFASs. Pd doping helps to improve Fe corrosion as well as to increase its electron-donating capacity (Quinn et al. 2009). A galvanic cell is formed with a catalytic amount of Pd (being less active) which attracts electrons towards itself (increase in electron density). This makes Fe to be more electron-deficient and thus its surface to be more

positively charged. Comparing the zeta potentials of nZVI and nZVI/Pd at the same operating pH of 5, Figure 3.14 shows an average potential of +2.3 for the former and +14.1 for the latter.

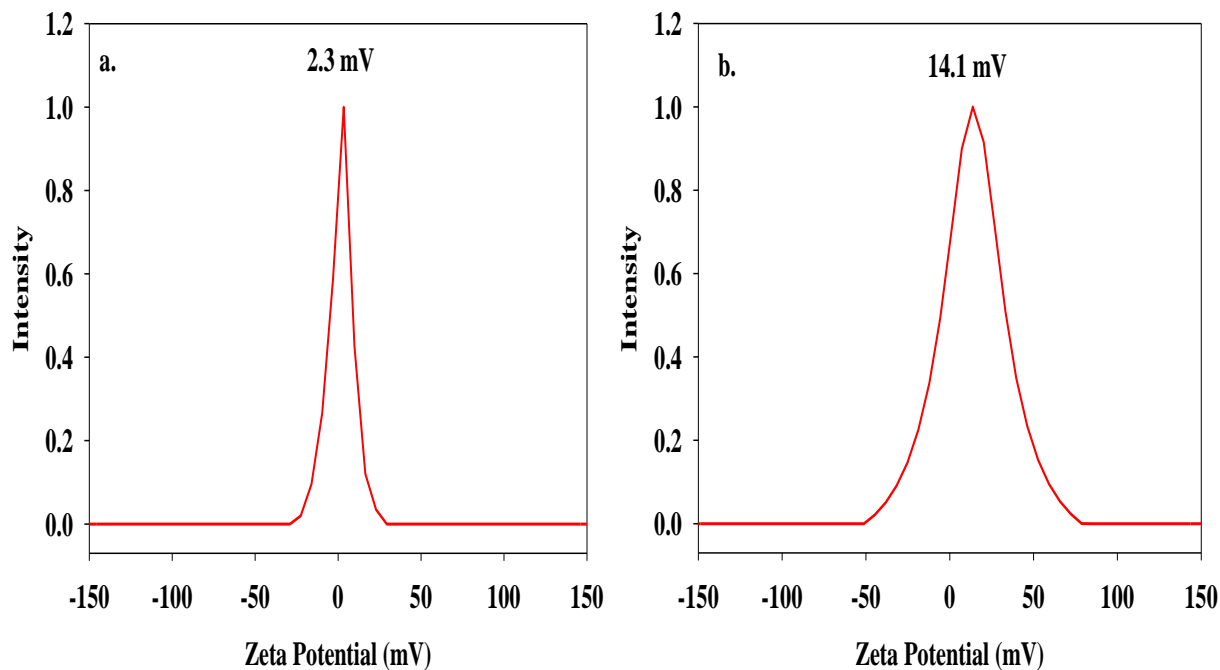


Figure 3.13 Zeta potential graphs of (a) nZVI and (b) nZVI/Pd

Investigating further, the Zeta potentials of both particles are analyzed at different pH conditions. Figure 3.14 shows that the zeta potential of nZVI was shifted towards positive side after Pd doping and thus overall, nZVI/Pd showed higher positive electrical potentials than nZVI over pH conditions. The point of zero charges of nZVI/Pd and nZVI were pH 6.2 and pH 5.1, respectively, below which the ZVI materials are positively charged.

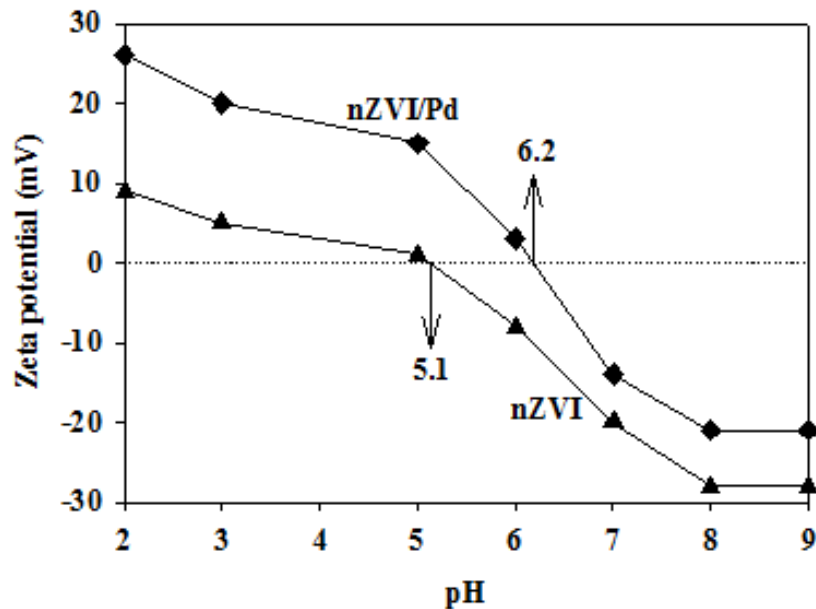


Figure 3.14 Zeta potential of nZVI and nZVI/Pd over pH.

As an anionic surfactant, PFOA has a negatively charged ionic headgroup (carboxylic) and a non-polar end that serves as tail (Gao and Chorover 2012; Du et al. 2014; C. Y. Tang et al. 2010; Villagrana, de Alda, and Barceló 2006). Since PFOA has a low pK_a at 2.3, it exists mainly as negatively charged ions under all the tested pH conditions (Goss 2008). Thus, PFOA is electrostatically attracted to positively charged nZVI/Pd via electrostatic attractions (Gao and Chorover 2012). The result shown in Figure 3.7 that PFOA showed better removal at lower pHs is in good agreement with nZVI/Pd having higher positive Zeta potential at lower pHs. The higher point of zero charge of nZVI/Pd at 6.2 than nZVI at 5.1 can also explain the result shown in Figure 3.6 that more PFOA was removed onto nZVI/Pd than nZVI under pH 5 where nZVI/Pd was positively charged while nZVI was more or less neutral.

Based on the discussion, the following are speculated to explain the overall PFOA removal onto nZVI/Pd. At low initial PFOA concentrations (less than 10 mg/L), adsorption is dominated by

covalent bonding, which can be explained with the somewhat flat slope isotherm, i.e., most of PFOA added tends to stay in the aqueous phase (Smith 1956; Hayward and Trapnell 1964). According to Ho and McKay (Ho and McKay 1998; Ho and McKay 1999) adsorption involving covalent interactions, known as chemisorption, typically follows pseudo-second-order kinetics, as also observed in this case (note Table 3.1).

Meanwhile, PFOA at high initial concentrations is expected to self-assemble. PFOA at concentrations of 15.7-157 mg/L (0.01-0.001 times less than its critical micellar concentration) was reported to form hemimicelles on adsorbent surfaces (Du et al. 2014). Hemi-micelles are typically formed by aggregation of hydrophobic tails of surfactant molecules (Du et al. 2014). The isotherm slope for such high initial PFOA concentrations becomes steep because surfactant-surfactant hydrophobic interactions start to occur, causing cooperative sorption in which added PFOA tends to preferentially partition into nZVI/Pd (Hinz 2001). This leads to formation of PFOA monolayer clusters on nZVI/Pd. Then, the plateau indicates the eventual formation of surfactant bilayers, above which all extra PFOA stays in water as shown in figure 3.15 below (Du et al. 2014; Gao and Chorover 2012).

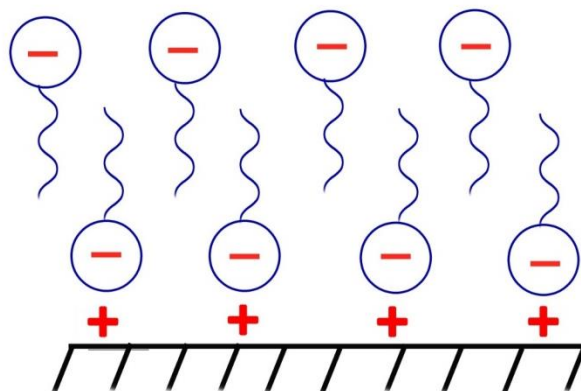


Figure 3.15 Schematic diagram of a surfactant bilayer on a positively charged surface.

The S-shaped isotherm or sigmoidal isotherm observed for the adsorption of PFOA onto nZVI/Pd was also reported for adsorption of many other anionic surfactants onto positively charged surfaces (Gao and Chorover 2012).

CHAPTER 5

Conclusion and future work

Palladium doped nZVI has properties that make able to decompose halogenated organic pollutants. PFOA is a persistent organic pollutant and has so far proven to be resistant to many conventional treatment methods at ambient conditions. Nanoscale ZVI/Pd appears (in theory) to be an attractive option for the treatment of PFOA contamination but hardly any studies have been published at this point so the objective of this study was to investigate this.

Initial tests did show that nZVI/Pd does remove PFOA from water with better efficiency at certain conditions such as low pH and higher loadings and was also more efficient than microscale ZVI and nZVI. All of these outcomes were expected and thought to be as a result of PFOA decomposition.

Where uncertainty arose was when we attempted to elucidate the mechanism of supposed decomposition reactions. Initially, the removal rate of PFOA increases with an increase in concentration which is contrary to what has typically been reported for the decomposition of organic contaminants. This, in conjunction with the fact none of the expected “degradation” by-products were detected by fluoride ion or mass spectrometry analysis led to the hypothesis that the likely pathway for PFOA removal in water by nZVI/Pd bimetallic particles might be due to adsorption and not decomposition as expected.

Further investigations showed that PFOA removal in the presence of nZVI/Pd was a better fit with pseudo-second-order adsorption kinetics which is an indication of chemical adsorption (chemisorption).

Electrostatic interactions between charged PFOA and nZVI/Pd and thus the removal of the former could be partially explained by Zeta potential variation over various pHs. PFOA removal via adsorption mechanism followed pseudo second order kinetics and the S-shaped adsorption isotherm followed Chapman model, indicating initial covalent interactions (a major characteristic of chemisorption) and then hydrophobic attractions to form PFOA monolayer clusters followed by PFOA surfactant bilayers.

In terms of recommendations, it is still not clear why nZVI/Pd, with its strong dehalogenation capability towards many halogenated compounds is not effective for PFOA decomposition. The answer may lie in the unique chemistry of PFOA and the C-F bonds in particular. This is an issue that needs to be thoroughly investigated.

While this study was able to postulate some theories as to the interactions between nZVI/Pd and PFOA, deeper studies using techniques like XRD and Fourier transform infrared (FTIR) are still needed in order to obtain a full understanding of the whole system.

Another possible area of investigation is the coupling of nZVI with common oxidants like peroxymonosulfate, persulfate and hydrogen peroxide or other less studied oxidants like perborate and periodate. Studies have shown that some systems containing different iron-based materials and some of the aforementioned oxidants have been effective at high pH and as such more work with nZVI and possibly activated carbon (to sequester PFOA and any possible reaction by-products) is needed.

References

- Agrawal, Abinash and Paul G. Tratnyek. 1995. "Reduction of Nitro Aromatic Compounds by Zero-Valent Iron Metal." *Environmental Science & Technology* 30 (1): 153-160.
- Alonso, Francisco, Irina P. Beletskaya, and Miguel Yus. 2002. "Metal-Mediated Reductive Hydrodehalogenation of Organic Halides." *Chemical Reviews* 102 (11): 4009-4092.
- Arvaniti, Olga S., Yuhoon Hwang, Henrik R. Andersen, Athanasios S. Stasinakis, Nikolaos S. Thomaidis, and Maria Aloupi. 2015. "Reductive Degradation of Perfluorinated Compounds in Water using mg-Aminoclay Coated Nanoscale Zero Valent Iron." *Chemical Engineering Journal* 262: 133-139.
- Baer, Donald R., Paul G. Tratnyek, You Qiang, James E. Amonette, John Linehan, Vaishnavi Sarathy, James T. Nurmi, Chongmin Wang, and Jiji Antony. 2012. "Synthesis, Characterization, and Properties of Zero-Valent Iron Nanoparticles." In *Environmental Applications of Nanomaterials: Synthesis, Sorbents and Sensors*, 49-86: World Scientific.
- Bao, Yueping, Junfeng Niu, Zesheng Xu, Ding Gao, Jianghong Shi, Xiaomin Sun, and Qingguo Huang. 2014. "Removal of Perfluorooctane Sulfonate (PFOS) and Perfluorooctanoate (PFOA) from Water by Coagulation: Mechanisms and Influencing Factors." *Journal of Colloid and Interface Science* 434: 59-64.
- Bautista, P., AF Mohedano, JA Casas, JA Zazo, and JJ Rodriguez. 2008. "An Overview of the Application of Fenton Oxidation to Industrial Wastewaters Treatment." *Journal of Chemical Technology and Biotechnology* 83 (10): 1323-1338.
- Benford, D., de J. Boer, A. Carere, di A. Domenico, N. Johansson, D. Schrenk, G. Schoeters, de P. Voogt, and E. Dellatte. 2008. "Opinion of the Scientific Panel on Contaminants in the Food Chain on Perfluorooctane Sulfonate (PFOS), Perfluorooctanoic Acid (PFOA) and their Salts." *EFSA Journal* (653): 1-1-131. <http://dare.uva.nl/record/299289>.
- Bigg, T. and SJ Judd. 2000. "Zero-Valent Iron for Water Treatment." *Environmental Technology* 21 (6): 661-670.
- Brillas, Enric, Eva Mur, Roser Sauleda, Laura Sanchez, Josa Peral, Xavier Domenech, and Juan Casado. 1998. "Aniline Mineralization by AOP's: Anodic Oxidation, Photocatalysis, Electro-Fenton and Photoelectro-Fenton Processes." *Applied Catalysis B: Environmental* 16 (1): 31-42. <http://www.sciencedirect.com/science/article/pii/S0926337397000593>.
- Carter, K. E. and J. Farrell. 2010. "Removal of Perfluorooctane and Perfluorobutane Sulfonate from Water Via Carbon Adsorption and Ion Exchange." *Separation Science and Technology* 45 (6): 762-767.
- Carter, Kimberly E. and James Farrell. 2008. "Oxidative Destruction of Perfluorooctane Sulfonate using Boron-Doped Diamond Film Electrodes." *Environmental Science & Technology* 42 (16): 6111-6115.
- Çeçen, Ferhan and Özgür Aktas. 2011. *Activated Carbon for Water and Wastewater Treatment: Integration of Adsorption and Biological Treatment* John Wiley & Sons.

- Chen, J. and P. Zhang. 2006. "Photodegradation of Perfluorooctanoic Acid in Water Under Irradiation of 254 Nm and 185 Nm Light by use of Persulfate." *Water Science and Technology* 54 (11-12): 317-325.
- Chen, Meng-Jia, Shang-Lien Lo, Yu-Chi Lee, and Chang-Chieh Huang. 2015. "Photocatalytic Decomposition of Perfluorooctanoic Acid by Transition-Metal Modified Titanium Dioxide." *Journal of Hazardous Materials* 288: 168-175.
- Choi, H., S. Agarwal, and S. R. Al-Abed. 2008. "Adsorption and Simultaneous Dechlorination of PCBs on GAC/Fe/Pd: Mechanistic Aspects and Reactive Capping Barrier Concept." *Environmental Science & Technology* 43 (2): 488-493.
- Choi, H. and S. R. Al-Abed. 2009. "PCB Congener Sorption to Carbonaceous Sediment Components: Macroscopic Comparison and Characterization of Sorption Kinetics and Mechanism." *Journal of Hazardous Materials* 165 (1-3): 860-866.
- Choi, H., S. R. Al-Abed, and S. Agarwal. 2009a. "Catalytic Role of Palladium and Relative Reactivity of Substituted Chlorines during Adsorption and Treatment of PCBs on Reactive Activated Carbon." *Environmental Science & Technology* 43 (19): 7510-7515.
- H Choi, SR Al-Abed, S Agarwal. 2009b. "Effects of Aging and Oxidation of Palladized Iron Embedded in Activated Carbon on the Dechlorination of 2-Chlorobiphenyl." *Environmental Science & Technology* 43 (11): 4137-4142.
- Crisp, T. M., E. D. Clegg, R. L. Cooper, W. P. Wood, D. G. Anderson, K. P. Baetcke, J. L. Hoffmann, M. S. Morrow, D. J. Rodier, and J. E. Schaeffer. 1998. "Environmental Endocrine Disruption: An Effects Assessment and Analysis." *Environmental Health Perspectives* 106 (Suppl 1): 11.
- da Silva-Rackov, Celyna KO, Wasiu A. Lawal, Prince A. Nfodzo, Marilda MGR Vianna, Claudio AO do Nascimento, and Hyeok Choi. 2016. "Degradation of PFOA by Hydrogen Peroxide and Persulfate Activated by Iron-Modified Diatomite." *Applied Catalysis B: Environmental* 192: 253-259.
- Dillert, R., D. Bahnemann, and H. Hidaka. 2007. "Light-Induced Degradation of Perfluorocarboxylic Acids in the Presence of Titanium Dioxide." *Chemosphere* 67 (4): 785-792.
- Dror, I., T. B. Moshe, and B. Berkowitz. 2009. "Use of Nanoparticles for Degradation of Water Contaminants in Oxidative and Reductive Reactions." ACS Publications, .
- Du, Ziwen, Shubo Deng, Yue Bei, Qian Huang, Bin Wang, Jun Huang, and Gang Yu. 2014. "Adsorption Behavior and Mechanism of Perfluorinated Compounds on various adsorbents—A Review." *Journal of Hazardous Materials* 274: 443-454. doi:<http://dx.doi.org/10.1016/j.jhazmat.2014.04.038>.
- Eilperin, Juliet. 2005. "Compound in Teflon a Likely Carcinogen." *Washington Post*: 4.
- Eskandarian, Mohammad Reza, Hyeok Choi, Mostafa Fazli, and Mohammad Hossein Rasoulifard. 2016. "Effect of UV-LED Wavelengths on Direct Photolytic and TiO₂ Photocatalytic Degradation of Emerging Contaminants in Water." *Chemical Engineering Journal* 300: 414-422.

- Farrell, James, Mark Kason, Nicos Melitas, and Tie Li. 2000. "Investigation of the Long-Term Performance of Zero-Valent Iron for Reductive Dechlorination of Trichloroethylene." *Environmental Science & Technology* 34 (3): 514-521.
- Fujii, S., C. Polprasert, S. Tanaka, P. H. L. NGUYEN, and QIU YONG. 2007. "New POPs in the Water Environment: Distribution, Bioaccumulation and Treatment of Perfluorinated Compounds-a Review Paper." *Journal of Water Supply: Research and Technology.AQUA* 56 (5): 313-326.
- Gao, Xiaodong and Jon Chorover. 2012. "Adsorption of Perfluorooctanoic Acid and Perfluorooctanesulfonic Acid to Iron Oxide Surfaces as Studied by Flow-through ATR-FTIR Spectroscopy." *Environmental Chemistry* 9 (2): 148-157.
- Gatto, Sara, Maurizio Sansotera, Federico Persico, Massimo Gola, Carlo Pirola, Walter Panzeri, Walter Navarrini, and Claudia L. Bianchi. 2015. "Surface Fluorination on TiO₂ Catalyst Induced by Photodegradation of Perfluorooctanoic Acid." *Catalysis Today* 241: 8-14.
- Ghauch, A. 2008. "Rapid Removal of Flutriafol in Water by Zero-Valent Iron Powder." *Chemosphere* 71 (5): 816-826.
- Giri, RR, H. Ozaki, T. Morigaki, S. Taniguchi, and R. Takanami. 2011. "UV Photolysis of Perfluorooctanoic Acid (PFOA) in Dilute Aqueous Solution." *Water Science and Technology* 63 (2): 276-282.
- Gladitz, M. 2014. *Science and Technology Against Microbial Pathogens : Research, Development and Evaluation*, edited by Antonio Mendez-Vilas. Singapore: World Scientific Publishing Co Pte Ltd.
- Hansen, KJ, HO Johnson, JS Eldridge, JL Butenhoff, and LA Dick. 2002. "Quantitative Characterization of Trace Levels of PFOS and PFOA in the Tennessee River." *Environmental Science & Technology* 36 (8): 1681-1685.
- Hansen, M. C., M. H. Børresen, M. Schlabach, and G. Cornelissen. 2010. "Sorption of Perfluorinated Compounds from Contaminated Water to Activated Carbon." *Journal of Soils and Sediments* 10 (2): 179-185.
- Hayward, David Oldham and Barry Maurice Waller Trapnell. 1964. *Chemisorption* Butterworths London.
- Hebert, G. N., M. A. Odom, P. S. Craig, D. L. Dick, and S. H. Strauss. 2002. "Method for the Determination of Sub-Ppm Concentrations of Perfluoroalkylsulfonate Anions in Water." *J. Environ. Monit.* 4 (1): 90-95.
- Hinz, Christoph. 2001. *Description of Sorption Data with Isotherm Equations*. Vol. 99. doi:[https://doi.org/10.1016/S0016-7061\(00\)00071-9](https://doi.org/10.1016/S0016-7061(00)00071-9).
- Ho, YS and Gordon McKay. 1998. "A Comparison of Chemisorption Kinetic Models Applied to Pollutant Removal on various Sorbents." *Process Safety and Environmental Protection* 76 (4): 332-340.
- Ho, Yuh-Shan and Gordon McKay. 1999. "Pseudo-Second Order Model for Sorption Processes." *Process Biochemistry* 34 (5): 451-465.

- Hoffman, K., T. F. Webster, M. G. Weisskopf, J. Weinberg, and V. M. Vieira. 2010. "Exposure to Polyfluoroalkyl Chemicals and Attention Deficit Hyperactivity Disorder in U.S. Children Aged 12-15 Years." *Environmental Health Perspectives*. doi:10.1289/ehp.1001898. www.refworks.com.
- Hogue, Cheryl. 2005a. "Dupont, EPA Settle." *Chemical & Engineering News* 83 (10).
- Hogue, Cheryl. 2005b. "PFOA Called Likely Human Carcinogen." *Chemical and Engineering News* 83 (27): 5.
- Hogue, Cheryl. 2006. "Pledges on PFOA-Eight Companies Agree to Cut Releases of Perfluorochemicals." *Chemical and Engineering News*, 10.
- Hori, H., A. Yamamoto, E. Hayakawa, S. Taniyasu, N. Yamashita, S. Kutsuna, H. Kiatagawa, and R. Arakawa. 2005. "Efficient Decomposition of Environmentally Persistent Perfluorocarboxylic Acids by use of Persulfate as a Photochemical Oxidant." *Environmental Science & Technology* 39 (7): 2383-2388.
- Hori, Hisao, Etsuko Hayakawa, Hisahiro Einaga, Shuzo Kutsuna, Kazuhide Koike, Takashi Ibusuki, Hiroshi Kiatagawa, and Ryuichi Arakawa. 2004. "Decomposition of Environmentally Persistent Perfluorooctanoic Acid in Water by Photochemical Approaches." *Environmental Science & Technology* 38 (22): 6118-6124.
- Hori, Hisao, Etsuko Hayakawa, Nobuyoshi Yamashita, Sachi Taniyasu, Fumiya Nakata, and Yoshimi Kobayashi. 2004. "High-Performance Liquid Chromatography with Conductimetric Detection of Perfluorocarboxylic Acids and Perfluorosulfonates." *Chemosphere* 57 (4): 273-282.
- Hornyak, Gabor L., John J. Moore, Harry F. Tibbals, and Joydeep Dutta. 2008. *Fundamentals of Nanotechnology* CRC press.
- Hotze, Matt and Greg Lowry. 2010. "Nanotechnology for Sustainable Water Treatment." In *Sustainable Water*, 138-164.
- Huang, Jiye, Xi Wang, Zhaoqi Pan, Xukai Li, Yu Ling, and Laisheng Li. 2016. "Efficient Degradation of Perfluorooctanoic Acid (PFOA) by Photocatalytic Ozonation." *Chemical Engineering Journal* 296: 329-334.
- Johnson, Timothy L., Michelle M. Scherer, and Paul G. Tratnyek. 1996. "Kinetics of Halogenated Organic Compound Degradation by Iron Metal." *Environmental Science & Technology* 30 (8): 2634-2640.
- Joo, Sung Hee and Frank Cheng. 2006. *Nanotechnology for Environmental Remediation* Springer Science & Business Media.
- Key, Blake D., Robert D. Howell, and Craig S. Criddle. 1997. "Fluorinated Organics in the Biosphere." *Environmental Science & Technology* 31 (9): 2445-2454. doi:10.1021/es961007c. <http://dx.doi.org/10.1021/es961007c>.
- Kissa, E. 1994. *Fluorinated Surfactants: Synthesis, Properties, Applications* M. Dekker. <http://books.google.com/books?id=vA9tAAAAMAJ>.

- Knepper, T. P. and F. T. Lange. 2011. *Polyfluorinated Chemicals and Transformation Products*. Vol. 17 Springer.
- Kuang, Ye, Qingping Wang, Zuliang Chen, Mallavarapu Megharaj, and Ravendra Naidu. 2013. "Heterogeneous Fenton-Like Oxidation of Monochlorobenzene using Green Synthesis of Iron Nanoparticles." *Journal of Colloid and Interface Science* 410: 67-73.
- Kudo, Naomi and Yoichi Kawashima. 2003. "Toxicity and Toxicokinetics of Perfluorooctanoic Acid in Humans and Animals." *The Journal of Toxicological Sciences* 28 (2): 49-57.
- Kudo, Naomi, Erika Suzuki-Nakajima, Atsushi Mitsumoto, and Yoichi Kawashima. 2006. "Responses of the Liver to Perfluorinated Fatty Acids with Different Carbon Chain Length in Male and Female Mice: In Relation to Induction of Hepatomegaly, Peroxisomal β -Oxidation and Microsomal 1-Acylglycerophosphocholine Acyltransferase." *Biological and Pharmaceutical Bulletin* 29 (9): 1952-1957.
- Lange, FT, C. Schmidt, and HJ Brauch. 2006. "Perfluoroalkylcarboxylates And-sulfonates." .
- Lau, C., K. Anitole, C. Hodes, D. Lai, A. Pfahles-Hutchens, and J. Seed. 2007. "Perfluoroalkyl Acids: A Review of Monitoring and Toxicological Findings." *Toxicological Sciences : An Official Journal of the Society of Toxicology* 99 (2): 366-394. doi:kfm128 [pii].
- Lee, Yu-Chi, Shang-Lien Lo, Pei-Te Chiueh, Yau-Hsuan Liou, and Man-Li Chen. 2010. "Microwave-Hydrothermal Decomposition of Perfluorooctanoic Acid in Water by Iron-Activated Persulfate Oxidation." *Water Research* 44 (3): 886-892.
- Li, Shaolin, Weile Yan, and Wei-xian Zhang. 2009. "Solvent-Free Production of Nanoscale Zero-Valent Iron (nZVI) with Precision Milling." *Green Chemistry* 11 (10): 1618-1626.
- Li, Xiaona, Shuo Chen, Xie Quan, and Yaobin Zhang. 2011. "Enhanced Adsorption of PFOA and PFOS on Multiwalled Carbon Nanotubes Under Electrochemical Assistance." *Environmental Science & Technology* 45 (19): 8498-8505.
- Li, Xiaoyun, Pengyi Zhang, Ling Jin, Tian Shao, Zhenmin Li, and Junjie Cao. 2012. "Efficient Photocatalytic Decomposition of Perfluorooctanoic Acid by Indium Oxide and its Mechanism." *Environmental Science & Technology* 46 (10): 5528-5534.
- Liang, C. and M. C. Lai. 2008. "Trichloroethylene Degradation by Zero Valent Iron Activated Persulfate Oxidation." *Environmental Engineering Science* 25 (7): 1071-1078.
- Liao, Zhaohui and James Farrell. 2009. "Electrochemical Oxidation of Perfluorobutane Sulfonate using Boron-Doped Diamond Film Electrodes." *Journal of Applied Electrochemistry* 39 (10): 1993-1999.
- Lien, Hsing-Lung and Wei-Xian Zhang. 2007. "Nanoscale Pd/Fe Bimetallic Particles: Catalytic Effects of Palladium on Hydrodechlorination." *Applied Catalysis B: Environmental* 77 (1): 110-116.
- Lifetime Health Advisories and Health Effects Support Documents for Perfluorooctanoic Acid and Perfluorooctane Sulfonate*. 2016. Washington: Federal Information & News Dispatch, Inc.

- Lin, Hui, Yujuan Wang, Junfeng Niu, Zhihan Yue, and Qingguo Huang. 2015. "Efficient Sorption and Removal of Perfluoroalkyl Acids (PFAAs) from Aqueous Solution by Metal Hydroxides Generated in Situ by Electrocoagulation." *Environmental Science & Technology* 49 (17): 10562-10569.
- Lindstrom, Andrew B., Mark J. Strynar, and E. Laurence Libelo. 2011. "Polyfluorinated Compounds: Past, Present, and Future." *Environmental Science and Technology* 44 (19): 7954-7961. *Environ. Sci. Technol.* 45, 19, 7954-7961.
- Liu, Yueqiang, Hyeok Choi, Dionysios Dionysiou, and Gregory V. Lowry. 2005. "Trichloroethene Hydrodechlorination in Water by Highly Disordered Monometallic Nanoiron." *Chemistry of Materials* 17 (21): 5315-5322.
- Liu, Yueqiang and Gregory V. Lowry. 2006. "Effect of Particle Age (Fe⁰ Content) and Solution pH on NZVI Reactivity: H₂ Evolution and TCE Dechlorination." *Environmental Science & Technology* 40 (19): 6085-6090.
- Liu, Yueqiang, Sara A. Majetich, Robert D. Tilton, David S. Sholl, and Gregory V. Lowry. 2005. "TCE Dechlorination Rates, Pathways, and Efficiency of Nanoscale Iron Particles with Different Properties." *Environmental Science & Technology* 39 (5): 1338-1345.
- Lowry, Gregory V. and Kathleen M. Johnson. 2004. "Congener-Specific Dechlorination of Dissolved PCBs by Microscale and Nanoscale Zerovalent Iron in a Water/Methanol Solution." *Environmental Science & Technology* 38 (19): 5208-5216. doi:10.1021/es049835q. <http://dx.doi.org/10.1021/es049835q>.
- Lutze, H., S. Panglisch, A. Bergmann, and T. Schmidt. 2012. "Treatment Options for the Removal and Degradation of Polyfluorinated Chemicals." *Polyfluorinated Chemicals and Transformation Products*: 103-125.
- Merino, Nancy, Yan Qu, Rula A. Deeb, Elisabeth L. Hawley, Michael R. Hoffmann, and Shaily Mahendra. 2016. "Degradation and Removal Methods for Perfluoroalkyl and Polyfluoroalkyl Substances in Water." *Environmental Engineering Science* 33 (9): 615-649.
- Mitchell, Shannon M., Mushtaque Ahmad, Amy L. Teel, and Richard J. Watts. 2013. "Degradation of Perfluorooctanoic Acid by Reactive Species Generated through Catalyzed H₂O₂ Propagation Reactions." *Environmental Science & Technology Letters* 1 (1): 117-121.
- Moody, Cheryl A. and Jennifer A. Field. 1999. "Determination of Perfluorocarboxylates in Groundwater Impacted by Fire-Fighting Activity." *Environmental Science & Technology* 33 (16): 2800-2806.
- Moody, Cheryl A., Wai Chi Kwan, Jonathan W. Martin, Derek CG Muir, and Scott A. Mabury. 2001. "Determination of Perfluorinated Surfactants in Surface Water Samples by Two Independent Analytical Techniques: Liquid Chromatography/Tandem Mass Spectrometry and ¹⁹F NMR." *Analytical Chemistry* 73 (10): 2200-2206.
- Moody, Cheryl A. and Jennifer A. Field. 2000. "Perfluorinated Surfactants and the Environmental Implications of their use in Fire-Fighting Foams." *Environmental Science & Technology* 34 (18): 3864-3870. doi:10.1021/es991359u. <http://dx.doi.org/10.1021/es991359u>.

- Moody, Cheryl A., Gretchen N. Hebert, Steven H. Strauss, and Jennifer A. Field. 2003. "Occurrence and Persistence of Perfluorooctanesulfonate and Other Perfluorinated Surfactants in Groundwater at a Fire-Training Area at Wurtsmith Air Force Base, Michigan, USA." *Journal of Environmental Monitoring* 5 (2): 341-345. <http://dx.doi.org/10.1039/B212497A>.
- Morales, J., R. Hutcheson, and I. F. Cheng. 2002. "Dechlorination of Chlorinated Phenols by Catalyzed and Uncatalyzed Fe (0) and mg (0) Particles." *Journal of Hazardous Materials* 90 (1): 97-108.
- Moriwaki, H., Y. Takagi, M. Tanaka, K. Tsuruho, K. Okitsu, and Y. Maeda. 2005. "Sonochemical Decomposition of Perfluorooctane Sulfonate and Perfluorooctanoic Acid." *Environmental Science & Technology* 39 (9): 3388-3392.
- Morrison, J. 2016a. "Perfluorinated Chemicals Taint Drinking Water (Vol 94, Pg 20, 2016)." *Chemical & Engineering News* 94 (23): 4-4.
- Morrison, Jessica. 2016b. "Chronic Exposure Limit Set for PFOA in Drinking Water." *Chemical & Engineering News*, May 23, 2016.
- Mudumbi, JBN, SKO Ntwampe, FM Muganza, and JO Okonkwo. 2014. "Perfluorooctanoate and Perfluorooctane Sulfonate in South African River Water." *Water Science and Technology* 69 (1): 185-194.
- Nägeli, KW. 1893. "Über Oligodynamische Erscheinungen in Lebenden Zellen. Neue Denkschr. Allgemein. Schweiz. Gesellsch. Ges." .
- Nassi, Marianna, Elena Sarti, Luisa Pasti, Annalisa Martucci, Nicola Marchetti, Alberto Cavazzini, Francesco Di Renzo, and Anne Galarneau. 2014. "Removal of Perfluorooctanoic Acid from Water by Adsorption on High Surface Area Mesoporous Materials." *Journal of Porous Materials* 21 (4): 423-432.
- Neta, P., R. E. Huie, and A. B. Ross. 1988. "Rate Constants for Reactions of Inorganic Radicals in Aqueous Solution." *Journal of Physical and Chemical Reference Data* 17: 1027.
- Nfodzo, Prince and Hyeok Choi. 2011a. "Sulfate Radicals Destroy Pharmaceuticals and Personal Care Products." *Environmental Engineering Science* 28 (8): 605-609. doi:10.1089/ees.2011.0045. <http://search.ebscohost.com/login.aspx?direct=true&db=a9h&AN=62970966&site=ehost-live>.
- Nfodzo, Prince and Hyeok Choi. 2011b. "Triclosan Decomposition by Sulfate Radicals: Effects of Oxidant and Metal Doses." *Chemical Engineering Journal* 174 (2-3): 629-634. doi:10.1016/j.cej.2011.09.076.
- Ochiai, Tsuyoshi, Yuichi Iizuka, Kazuya Nakata, Taketoshi Murakami, Donald A. Tryk, Akira Fujishima, Yoshihiro Koide, and Yuko Morito. 2011. "Efficient Electrochemical Decomposition of Perfluorocarboxylic Acids by the use of a Boron-Doped Diamond Electrode." *Diamond and Related Materials* 20 (2): 64-67.
- Ochiai, Tsuyoshi, Hirofumi Moriyama, Kazuya Nakata, Taketoshi Murakami, Yoshihiro Koide, and Akira Fujishima. 2011. "Electrochemical and Photocatalytic Decomposition of Perfluorooctanoic

- Acid with a Hybrid Reactor using a Boron-Doped Diamond Electrode and TiO₂ Photocatalyst." *Chemistry Letters* 40 (7): 682-683.
- Ochoa-Herrera, V., R. Sierra-Alvarez, A. Somogyi, N. E. Jacobsen, V. H. Wysocki, and J. A. Field. 2008. "Reductive Defluorination of Perfluorooctane Sulfonate." *Environmental Science & Technology* 42 (9): 3260-3264.
- Ochoa-Herrera, Valeria Lourdes. 2008. *Removal of Perfluorooctane Sulfonate (PFOS) and Related Compounds from Industrial Effluents* The University of Arizona.
- Ochoa-Herrera, Valeria and Reyes Sierra-Alvarez. 2008. "Removal of Perfluorinated Surfactants by Sorption Onto Granular Activated Carbon, Zeolite and Sludge." *Chemosphere* 72 (10): 1588-1593. doi:10.1016/j.chemosphere.2008.04.029.
- O'Hagan, David. 2008. "Understanding Organofluorine Chemistry. an Introduction to the C–F Bond." *Chemical Society Reviews* 37 (2): 308-319.
- Orth, W. Scott and Robert W. Gillham. 1995. "Dechlorination of Trichloroethene in Aqueous Solution using Fe⁰." *Environmental Science & Technology* 30 (1): 66-71.
- Pabon, M. and JM Corpart. 2002. "Fluorinated Surfactants: Synthesis, Properties, Effluent Treatment." *Journal of Fluorine Chemistry* 114 (2): 149-156.
- Panchangam, Sri Chandana, Angela Yu-Chen Lin, Khaja Lateef Shaik, and Cheng-Fang Lin. 2009. "Decomposition of Perfluorocarboxylic Acids (As) by Heterogeneous Photocatalysis in Acidic Aqueous Medium." *Chemosphere* 77 (2): 242-248.
- Park, Hyunwoong, Chad D. Vecitis, Jie Cheng, Wonyong Choi, Brian T. Mader, and Michael R. Hoffmann. 2009. "Reductive Defluorination of Aqueous Perfluorinated Alkyl Surfactants: Effects of Ionic Headgroup and Chain Length." *The Journal of Physical Chemistry A* 113 (4): 690-696.
- Park, Hyunwoong, Chad D. Vecitis, Jie Cheng, Nathan F. Dalleska, Brian T. Mader, and Michael R. Hoffmann. 2011. "Reductive Degradation of Perfluoroalkyl Compounds with Aquated Electrons Generated from Iodide Photolysis at 254 Nm." *Photochemical & Photobiological Sciences* 10 (12): 1945-1953.
- Park, Saerom, Jenny E. Zenobio, and Linda S. Lee. 2018. "Perfluorooctane Sulfonate (PFOS) Removal with Pd⁰/nFe⁰ Nanoparticles: Adsorption Or Aqueous Fe-Complexation, Not Transformation?" *Journal of Hazardous Materials* 342: 20-28.
- Peden-Adams, Margie M., Joyce E. Stuckey, Kristen M. Gaworecki, Jennifer Berger-Ritchie, Kathy Bryant, Patrick G. Jodice, Thomas R. Scott, Joseph B. Ferrario, Bing Guan, and Craig Vigo. 2009. "Developmental Toxicity in White Leghorn Chickens Following in Ovo Exposure to Perfluorooctane Sulfonate (PFOS)." *Reproductive Toxicology* 27 (3): 307-318.
- Pignatello, J. J., E. Oliveros, and A. MacKay. 2006. "Advanced Oxidation Processes for Organic Contaminant Destruction Based on the Fenton Reaction and Related Chemistry." *Critical Reviews in Environmental Science and Technology* 36 (1): 1-84.

- Poboży, Ewa, Edyta Król, Lena Wójcik, Mariusz Wachowicz, and Marek Trojanowicz. 2011. "HPLC Determination of Perfluorinated Carboxylic Acids with Fluorescence Detection." *Microchimica Acta* 172 (3-4): 409-417.
- Qu, Yan, Chao-Jie Zhang, Pei Chen, Qi Zhou, and Wei-Xian Zhang. 2014. "Effect of Initial Solution pH on Photo-Induced Reductive Decomposition of Perfluorooctanoic Acid." *Chemosphere* 107: 218-223.
- Qu, Yan, Chaojie Zhang, Fei Li, Xiaowen Bo, Guangfu Liu, and Qi Zhou. 2009. "Equilibrium and Kinetics Study on the Adsorption of Perfluorooctanoic Acid from Aqueous Solution Onto Powdered Activated Carbon." *Journal of Hazardous Materials* 169 (1): 146-152.
- Qu, Yan, Chaojie Zhang, Fei Li, Jing Chen, and Qi Zhou. 2010. "Photo-Reductive Defluorination of Perfluorooctanoic Acid in Water." *Water Research* 44 (9): 2939-2947.
- Quinn, J., D. Elliott, S. O'Hara, and A. Billow. 2009. "Use of Nanoscale Iron and Bimetallic Particles for Environmental Remediation: A Review of Field-Scale Applications." *Environmental Applications of Nanoscale and Microscale Reactive Metal Particles, Copyright: 263-285.*
- Quinn, J., C. Geiger, C. Clausen, K. Brooks, C. Coon, S. O'Hara, T. Krug, D. Major, W. S. Yoon, and A. Gavaskar. 2005. "Field Demonstration of DNAPL Dehalogenation using Emulsified Zero-Valent Iron." *Environmental Science & Technology* 39 (5): 1309-1318.
- Rayne, S. and K. Forest. 2009. "Perfluoroalkyl Sulfonic and Carboxylic Acids: A Critical Review of Physicochemical Properties, Levels and Patterns in Waters and Wastewaters, and Treatment Methods." *Journal of Environmental Science and Health Part A* 44 (12): 1145-1199.
- Reisch, Marc S. February 13, 2017. "DuPont and Chemours Settle PFOA Suits." *Chemical and Engineering News, C&EN*. <http://cen.acs.org/articles/95/web/2017/02/DuPont-Chemours-settle-PFOA-suits.html>.
- Reisch, Marc S. 2015. "DuPont Loses First PFOA Trial in Ohio." *Chemical and Engineering News, C&EN* 93: 20-21.
- Renner, R. 2001. "Growing Concern Over Perfluorinated Chemicals." *Environmental Science & Technology* 35 (7): 154-160.
- Ritter, S. K. 2010. "Fluorochemicals Go Short." *Chemical & Engineering News* 88 (5): 12-17.
- Roberts, ALynn, Lisa A. Totten, William A. Arnold, David R. Burris, and Timothy J. Campbell. 1996. "Reductive Elimination of Chlorinated Ethylenes by Zero-Valent Metals." *Environmental Science and Technology* 30 (8).
- Rosenfeldt, E. J. and K. G. Linden. 2004. "Degradation of Endocrine Disrupting Chemicals Bisphenol A, Ethinyl Estradiol, and Estradiol during UV Photolysis and Advanced Oxidation Processes." *Environmental Science & Technology* 38 (20): 5476-5483.
- Saif, Sadia, Arifa Tahir, and Yongsheng Chen. 2016. "Green Synthesis of Iron Nanoparticles and their Environmental Applications and Implications." *Nanomaterials* 6 (11): 209.

- Saito, N., K. Harada, K. Inoue, K. Sasaki, T. Yoshinaga, and A. Koizumi. 2004. "Perfluorooctanoate and Perfluorooctane Sulfonate Concentrations in Surface Water in Japan." *Journal of Occupational Health* 46 (1): 49-59.
- Scott, Brian F., Cheryl A. Moody, Christine Spencer, Jeffrey M. Small, Derek CG Muir, and Scott A. Mabury. 2006. "Analysis for Perfluorocarboxylic Acids/Anions in Surface Waters and Precipitation using GC– MS and Analysis of PFOA from Large-Volume Samples." *Environmental Science & Technology* 40 (20): 6405-6410.
- Shan, Guobin, S. Yan, RD Tyagi, Rao Y. Surampalli, and Tian C. Zhang. 2009. "Applications of Nanomaterials in Environmental Science and Engineering." *Practice Periodical of Hazardous, Toxic, and Radioactive Waste Management* 13 (2): 110-119.
- Shao, Tian, Pengyi Zhang, Ling Jin, and Zhenmin Li. 2013. "Photocatalytic Decomposition of Perfluorooctanoic Acid in Pure Water and Sewage Water by Nanostructured Gallium Oxide." *Applied Catalysis B: Environmental* 142: 654-661.
- Skutlarek, D., M. Exner, and H. Farber. 2006. "Perfluorinated Surfactants in Surface and Drinking Waters." *Environ Sci Pollut Res Int* 13 (5): 299-307. <http://ukpmc.ac.uk/abstract/MED/17067024>.
- Smith, Joseph Mauk. 1956. "Chemical Engineering Kinetics." .
- Society, American Chemical. 2005. "EPA Issues Draft Risk Assessment on PFOA." *Chemical & Engineering News*, January 17 2005, 28.
- Song, Chao, Peng Chen, Chunying Wang, and Lingyan Zhu. 2012. "Photodegradation of Perfluorooctanoic Acid by Synthesized TiO₂–MWCNT Composites Under 365 Nm UV Irradiation." *Chemosphere* 86 (8): 853-859.
- Song, Zhou, Heqing Tang, Nan Wang, and Lihua Zhu. 2013. "Reductive Defluorination of Perfluorooctanoic Acid by Hydrated Electrons in a Sulfite-Mediated UV Photochemical System." *Journal of Hazardous Materials* 262: 332-338.
- Stefaniuk, Magdalena, Patryk Oleszczuk, and Yong Sik Ok. 2016. "Review on Nano Zerovalent Iron (nZVI): From Synthesis to Environmental Applications." *Chemical Engineering Journal* 287: 618-632.
- Stein, Cheryl R., David A. Savitz, and Marcelle Dougan. 2009. "Serum Levels of Perfluorooctanoic Acid and Perfluorooctane Sulfonate and Pregnancy Outcome." *American Journal of Epidemiology* 170 (7): 837-846. doi:10.1093/aje/kwp212.
- Stroo, H., C. H. Ward, and B. C. Alleman. 2010. *In Situ Remediation of Chlorinated Solvent Plumes* Springer Verlag.
- Takagi, Sokichi, Fumie Adachi, Keiichi Miyano, Yoshihiko Koizumi, Hidetsugu Tanaka, Mayumi Mimura, Isao Watanabe, Shinsuke Tanabe, and Kurunthachalam Kannan. 2008. "Perfluorooctanesulfonate and Perfluorooctanoate in Raw and Treated Tap Water from Osaka, Japan." *Chemosphere* 72 (10): 1409-1412. doi:10.1016/j.chemosphere.2008.05.034.

- Takino, Masahiko, Shigeki Daishima, and Taketoshi Nakahara. 2003. "Liquid Chromatography/Mass Spectrometric Determination of Patulin in Apple Juice using Atmospheric Pressure Photoionization." *Rapid Communications in Mass Spectrometry* 17 (17): 1965-1972.
- Tang, Chuyang Y., Q. Shiang Fu, Dawen Gao, Craig S. Criddle, and James O. Leckie. 2010. "Effect of Solution Chemistry on the Adsorption of Perfluorooctane Sulfonate Onto Mineral Surfaces." *Water Research* 44 (8): 2654-2662.
- Tang, Chuyang Y., Q. Shiang Fu, AP Robertson, Craig S. Criddle, and James O. Leckie. 2006. "Use of Reverse Osmosis Membranes to Remove Perfluorooctane Sulfonate (PFOS) from Semiconductor Wastewater." *Environmental Science & Technology* 40 (23): 7343-7349.
- Tang, Heqing, Qingqing Xiang, Min Lei, Jingchun Yan, Lihua Zhu, and Jing Zou. 2012. "Efficient Degradation of Perfluorooctanoic Acid by UV–Fenton Process." *Chemical Engineering Journal* 184: 156-162.
- Taniyasu, Sachi, Kurunthachalam Kannan, Yuichi Horii, Nobuyasu Hanari, and Nobuyoshi Yamashita. 2003. "A Survey of Perfluorooctane Sulfonate and Related Perfluorinated Organic Compounds in Water, Fish, Birds, and Humans from Japan." *Environmental Science & Technology* 37 (12): 2634-2639. doi:10.1021/es0303440. <http://dx.doi.org/10.1021/es0303440>.
- Teng, Jiuwei, Shuze Tang, and Shiyi Ou. 2009. "Determination of Perfluorooctanesulfonate and Perfluorooctanoate in Water Samples by SPE-HPLC/Electrospray Ion Trap Mass Spectrometry." *Microchemical Journal* 93 (1): 55-59.
- Thompson, Jack, Geoff Eaglesham, Julien Reungoat, Yvan Poussade, Michael Bartkow, Michael Lawrence, and Jochen F. Mueller. 2011. "Removal of PFOS, PFOA and Other Perfluoroalkyl Acids at Water Reclamation Plants in South East Queensland Australia." *Chemosphere* 82 (1): 9-17. doi:10.1016/j.chemosphere.2010.10.040.
- Toda, Corporation. "What is RNIP?".
- Trojanowicz, Marek, Anna Bojanowska-Czajka, Iwona Bartosiewicz, and Krzysztof Kulisa. 2018. "Advanced Oxidation/Reduction Processes Treatment for Aqueous Perfluorooctanoate (PFOA) and Perfluorooctanesulfonate (PFOS)—A Review of Recent Advances." *Chemical Engineering Journal* 336: 170-199.
- Urtiaga, Ane, Carolina Fernández-González, Sonia Gómez-Lavín, and Inmaculada Ortiz. 2015. "Kinetics of the Electrochemical Mineralization of Perfluorooctanoic Acid on Ultrananocrystalline Boron Doped Conductive Diamond Electrodes." *Chemosphere* 129: 20-26.
- Vecitis, C. D., H. Park, J. Cheng, B. T. Mader, and M. R. Hoffmann. 2008. "Kinetics and Mechanism of the Sonolytic Conversion of the Aqueous Perfluorinated Surfactants, Perfluorooctanoate (PFOA), and Perfluorooctane Sulfonate (PFOS) into Inorganic Products." *The Journal of Physical Chemistry A* 112 (18): 4261-4270.
- Vecitis, Chad D., Hyunwoong Park, Jie Cheng, Brian T. Mader, and Michael R. Hoffmann. 2009. "Treatment Technologies for Aqueous Perfluorooctanesulfonate (PFOS) and Perfluorooctanoate (PFOA)." *Frontiers of Environmental Science & Engineering in China* 3 (2): 129-151.

- Vellanki, Bhanu Prakash, Bill Batchelor, and Ahmed Abdel-Wahab. 2013. "Advanced Reduction Processes: A New Class of Treatment Processes." *Environmental Engineering Science* 30 (5): 264-271.
- Villagrasa, Marta, Maria López de Alda, and Damià Barceló. 2006. "Environmental Analysis of Fluorinated Alkyl Substances by Liquid Chromatography–(Tandem) Mass Spectrometry: A Review." *Analytical and Bioanalytical Chemistry* 386 (4): 953-972.
- Wang, Yuan, Pengyi Zhang, Gang Pan, and Hao Chen. 2008. "Ferric Ion Mediated Photochemical Decomposition of Perfluorooctanoic Acid (PFOA) by 254 Nm UV Light." *Journal of Hazardous Materials* 160 (1): 181-186.
- Wei, Jianjun, Xinhua Xu, Yong Liu, and Dahui Wang. 2006. "Catalytic Hydrodechlorination of 2, 4-Dichlorophenol Over Nanoscale Pd/Fe: Reaction Pathway and some Experimental Parameters." *Water Research* 40 (2): 348-354.
- Williams, Linda D. and Wade Adams. 2006. *Nanotechnology Demystified* McGraw Hill Professional.
- Wu, Siyang and Hyeok Choi. 2016. "Interpreting Unique Colloidal Response of TiO₂ Nanomaterials to Controlled Sonication for Understanding of their Assembly Configuration in Water." *Water Science and Technology: Water Supply* 16 (6): 1768-1775.
- Xiao, Feng, Matt F. Simcik, and John S. Gulliver. 2013. "Mechanisms for Removal of Perfluorooctane Sulfonate (PFOS) and Perfluorooctanoate (PFOA) from Drinking Water by Conventional and Enhanced Coagulation." *Water Research* 47 (1): 49-56.
- Yamamoto, Takashi, Yukio Noma, Shin-ichi Sakai, and Yasuyuki Shibata. 2007. "Photodegradation of Perfluorooctane Sulfonate by UV Irradiation in Water and Alkaline 2-Propanol." *Environmental Science & Technology* 41 (16): 5660-5665.
- Yu, Qiang, Ruiqi Zhang, Shubo Deng, Jun Huang, and Gang Yu. 2009. "Sorption of Perfluorooctane Sulfonate and Perfluorooctanoate on Activated Carbons and Resin: Kinetic and Isotherm Study." *Water Research* 43 (4): 1150-1158.
- Zainuddin, Khairunnisa, Mohamad Pauzi Zakaria, Najat Ahmed Al-Odaini, Alireza Riyahi Bakhtiari, and Puziah Abdul Latif. 2012. "Perfluorooctanoic Acid (PFOA) and Perfluorooctane Sulfonate (PFOS) in Surface Water from the Langat River, Peninsular Malaysia." *Environmental Forensics* 13 (1): 82-92.
- Zhang, Chaojie, Yan Qu, Xiaoyun Zhao, and Qi Zhou. 2015. "Photoinduced Reductive Decomposition of Perfluorooctanoic Acid in Water: Effect of Temperature and Ionic Strength." *CLEAN–Soil, Air, Water* 43 (2): 223-228.
- Zhang, W., C. B. Wang, and H. L. Lien. 1998. "Treatment of Chlorinated Organic Contaminants with Nanoscale Bimetallic Particles." *Catalysis Today* 40 (4): 387-395.
- Zhang, Ze, Jie-Jie Chen, Xian-Jin Lyu, Hao Yin, and Guo-Ping Sheng. 2014. "Complete Mineralization of Perfluorooctanoic Acid (PFOA) by Γ -Irradiation in Aqueous Solution." *Scientific Reports* 4: 7418.

- Zhao, Baoxiu. 2011. "Photocatalytic Degradation of Perfluorooctanoic Acid (PFOA) with B-Ga₂O₃ at Reductive Atmosphere." *Progress in Environmental Science and Technology* 3: 152; 152-156; 156.
- Zhao, Lixia, Jingna Bian, Yahui Zhang, Lingyan Zhu, and Zhengtao Liu. 2014. "Comparison of the Sorption Behaviors and Mechanisms of Perfluorosulfonates and Perfluorocarboxylic Acids on Three Kinds of Clay Minerals." *Chemosphere* 114: 51-58.
- Zhuang, Yuan, Sungwoo Ahn, Angelia L. Seyfferth, Yoko Masue-Slowey, Scott Fendorf, and Richard G. Luthy. 2011. "Dehalogenation of Polybrominated Diphenyl Ethers and Polychlorinated Biphenyl by Bimetallic, Impregnated, and Nanoscale Zerovalent Iron." *Environmental Science & Technology* 45 (11): 4896-4903.